Studies on the Delay Mechanism of Runoff to Snowmelt

by
Mutumi NOMURA
野 村 睦
The Institute of Low Temperature Science

Received December 1994

Abstract

In order to investigate the mechanism of the meltwater infiltration through a snowpack as a snowmelt runoff process, field observations were made at a watershed, 1.3 km^2 in area, in northern Hokkaido, Japan.

The time of peak runoff became earlier with decreasing snow depth and it differed yearly. The yearly difference was about 2 hours when the snow depth was 100 cm. The discharge at the bottom of the snowpack was observed with a large snow lysimeter. The result showed the yearly difference in the apparent infiltration speed which was consistent with that in runoff. The speed for the snowpack with several ice layers was about 30 cm h^{-1} and 15 cm h^{-1} for the snowpack with a few ice layers when the daily snowmelt was 20 mm.

The author considered that meltwater concentrated at the ice layers and the concentrated meltwater flowed at a larger speed. The concentrated flow was observed with a lysimeter consisting of 100 compartments of 200 cm^2. At a certain compartment, the daily discharge exceed over 30 times of an average snowmelt. We classified meltwater flow to three groups : 1) small number of high concentrated flows; 2) relatively large number of low concentrated flows; 3) many non-concentrated flows. The simulation of the infiltration through the snowpack considering these meltwater flows reproduced the observed discharge at the bottom of snowpack and yearly difference in the infiltration speed better than that without concentration.

The travel time of the infiltration in the snowpack on a slope was close to that on a flat site because the meltwater moved downslope on the ice layer much faster than vertical and the distance was small. The infiltration on a slope can be treated in a similar manner to that on a flat site. The simulation of the infiltration in the snowpack is extended to the whole watershed with a kinematic wave method for slope and stream flows. The simulation reproduced the observed discharge and the yearly difference in the runoff response very well.

* Contribution No. 3813 from the Institute of Low Temperature Science
北海道大学審査学位論文

Contents

I. Introduction

Most mountain areas in Japan are covered with thick snowpacks in winter. In spring the snow melts and heavy runoff occurs. Studies on snowmelt runoff have been made for the utilization of water resources and the prevention of floods. Snowmelt runoff is interesting for hydrology due to the unique process in which most precipitation in winter is stored as a snowpack temporarily and discharged in spring.

It is important to consider the snowpack as a source of river water as well as the medium in which the meltwater infiltrates before percolating into the soil. Due to the above process, the response of snowmelt runoff of a river is delayed in comparison with the case of rain, when there is no snow in the watershed. On a fine day, the peak snowmelt rate appears at about noon, and the peak discharge in the river occurs in evening or at night. The time lag between both events can be separated into the travel times in the snowpack and soil. Kobayashi and Motoyama (1986) showed that the infiltration in the snowpack took about one third or half the time from the peak snowmelt event to runoff in headwaters when the snow depth was 100 cm. The infiltration through the snowpack is an important process for snowmelt runoff.

Theoretical or observational investigations on the infiltration through the snowpack (Wakahama 1963, Yosida 1965, Wakahama et al. 1968) and the measurements of the downward speed of meltwater (Wakahama 1968, Fujino 1968, Kobayashi 1973) were made in the early stage of the studies. After that, Colbeck (1972) proposed a gravity flow theory in which the infiltration in the snowpack was mainly governed by gravity because the capillary pressure gradient in the snowpack was not important due to the coarse snow grains in the melting snowpack. Measurements of capillary pressure (Wankiewicz 1978, Jordan 1983a) and simulations (Jordan 1983b, Dunne et al. 1976) supported the gravity flow theory when the structure of the snowpack was homogeneous. However, when a snowpack is formed of many stratified layers, the infiltration in the snowpack does not occur uniformly. Lately, observations of non-uniform infiltration (Marsh and Woo 1984a, 1985) and simulations considering non-uniformity (Colbeck 1979, Marsh and Woo 1984b, 1985, Furbish 1988) were made. However, the relationship between the stratification of a snowpack and non-uniform infiltration has not been understood well. The infiltration in a snowpack is an important process for snowmelt runoff, as mentioned above, but considerations of the infiltration to the river runoff have not been made.

The main issue in this paper is to consider the infiltration through the snowpack as a delayed process of runoff. The primary purposes are (1) to clarify the mechanism of infiltration through the snowpack and to develop a model, and (2) to describe the difference in the infiltration owing to the change in altitude or topography and apply it to a runoff model for the whole watershed.

II. Study area and instruments

Field observations were made at an experimental watershed (Figure 1) located in Moshiri, northern Hokkaido, Japan, at 44°23'N, 142°17'E. The area of this watershed is 1.3 km². The elevation ranges from 290 m to 540 m a.s.l., and the area under 400 m occupies about 70 % of the entire watershed (Figure 2). The vegetation cover is a mixed forest with broad-leaved trees, coniferous trees and dense bamboo bush undergrowth. In winter, it is covered with snow as deep as about 2 m and the mean temperature is about −10°C. The snowy season is nearly six months, and the snow cover usually disappears in early May. This watershed is in one of the coldest and most snowy areas in Japan.

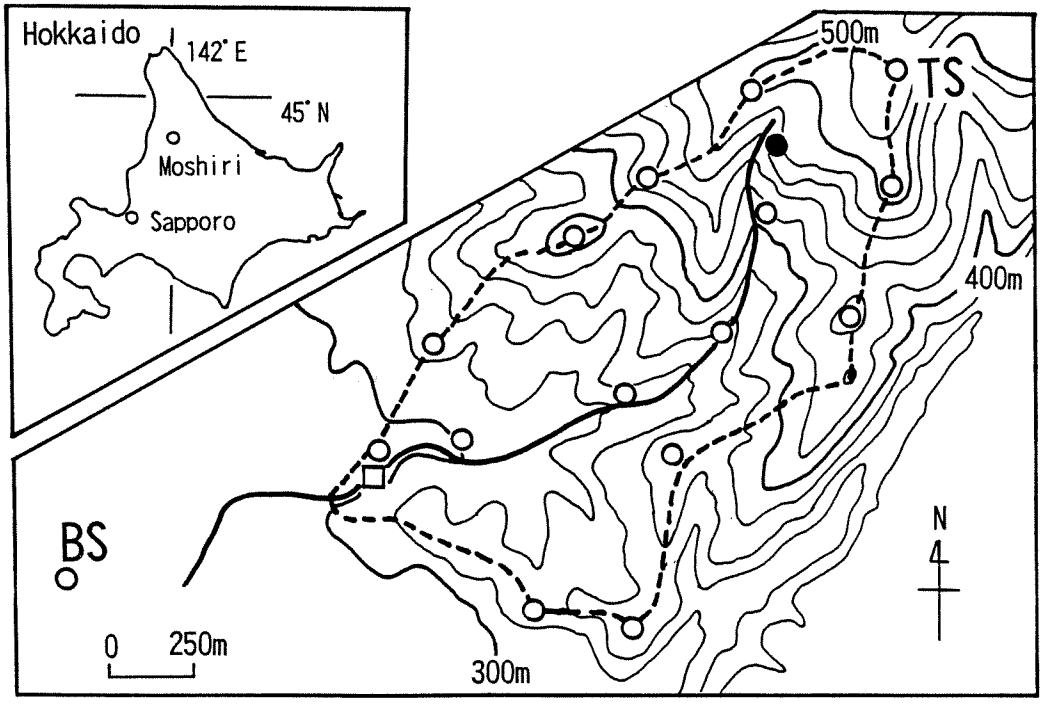

Figure 1 Location map of the experimental watershed. Broken line is the divided. BS (base station) and TS (top station) are the main observational stations. Open circles : snow depth, snow water equivalent and the lowering of the snow surface were measured. Solid circle : tracer test for the snowpack was made. Square : flow rate was measured.

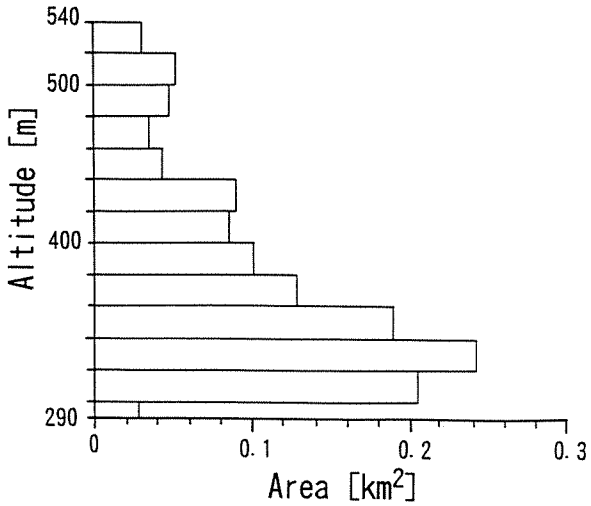

Figure 2 Altitudinal distribution of area of the watershed.

Observations were made in four snowmelt seasons (1989, 1990, 1991 and 1992). In this study, the data obtained in the active snowmelt season is mainly used. The active snowmelt season is defined here as the period in which the entire watershed is covered with snow and the particles of the snowpack are granular. In this season, meltwater discharges from the bottom of the snowpack without storage in the snowpack, then active discharge in a river runoff occurs on fine days. Before this season, when snowmelt at the snow surface occurs, the discharge at the bottom of the snowpack does not occur or is small due to the high water retention capacity of the snowpack. After this season, the runoff tends to decrease due to the increase of snow free area in the watershed.

The top of the watershed and the observatory near the outlet were the main observational sites. This paper names the former the top station (TS) and the latter the base station (BS). The elements of the observations are described below. These observations, except (7) and (8), were made every year.

(1) Snow depth was measured with a rod at seven or fifteen sites (open circles in Figure 1) in the watershed in early snowmelt season. After that, it was estimated through the lowering of snow surface measured with snow stakes.

(2) Snow water equivalent was measured with a snow sampler at seven or fifteen sites (open circles in Figure 1) in the watershed in early snowmelt season.

(3) Snowmelt was estimated through the lowering of snow surface and surface density at the base and top stations, and at seven or fifteen sites (open circles in Figure 1) in the watershed. At the base and the top stations, the heat balance method was also used to estimate snowmelt.

(4) Discharge at the bottom of the snowpack was measured with snow lysimeters at the base station and the top station.
(5) Discharge in the river was obtained with a weir at the outlet of the watershed (square in Figure 1).
(6) Snow pit observations were made several times during snowmelt season at the base and the top stations in order to describe the stratification and measure the grain size and density profiles.
(7) Tracer tests were made with dye in order to examine meltwater movement in the snowpack at a slope at an altitude of 470 m a.s.l. (solid circle in Figure 1) and the top of the watershed in 1992.
(8) Concentrated flow of meltwater in the snowpack was observed with a multi-compartment lysimeter at the base station in 1991 and 1992. The details of the observation will be described in chapter IV-3.

Heat balance at snow surface in snowmelt season is written as,

$$QM = QN + QS + QL, \tag{1}$$

where QM is the energy for snowmelt, QN net radiation, QS sensible heat flux, and QL latent heat flux. QN was measured, and QS and QL were estimated by the following empirical formulas (Ishikawa et al., 1982) which were obtained at the base station,

$$QS = K_s(T_1 - T_0)V_1, \tag{2}$$

$$QL = K_l(e_1 - e_0)V_1, \tag{3}$$

where T_1, e_1 and V_1 are air temperature, vapour pressure and wind speed at the height of 1 m above the snow surface, respectively, and T_0 is surface temperature and e_0 is the vapour pressure at the snow surface. K_s and K_l are bulk coefficients for heat and vapour transfers, and K_s is 0.26 and K_l is 0.69×10^{-3}. This formulas give QS and QL as the unit of ly hr^{-1}. According to Motoyama (1986), these formulas were applicable in the entire watershed, so the formulas were used for the estimation at the top station.

A snow lysimeter was installed at the ground surface, and snow was allowed to accumulate naturally. Figure 3 is a schematic diagram of the lysimeter. It has an area of 13 m^2 (3.6 m$\times$3.6 m). A lysimeter of about 1 m^2 in area can often measure the discharge erroneously due to non-uniform infiltration in the snowpack. However, the present larger lysimeter can measure representative discharge more accurately because the errors by the 'edge effect' due to non-uniform infiltration become smaller. The meltwater drained from the bottom of the snowpack into the lysimeter and was routed by a pipe to a tipping bucket gauge. The bucket volume is 500 ml, which corresponded to 0.04 mm of meltwater yield. This study calls this lysimeter the large lysimeter (L.L.) in order to distinguish it from the lysimeter described in chapter IV-3.

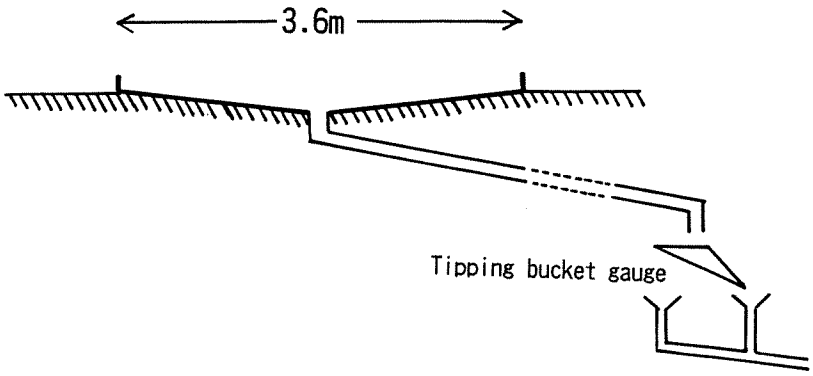

Figure 3 Schematic diagram of the large lysimeter.

III. Runoff in snowmelt season

Snowpack may store the meltwater temporarily, and the infiltration through the snowpack delays the discharge into a river. This chapter discusses the storage in the snowpack through water balance in the watershed and the delay of daily peak runoff.

1. *Water balance*

1) *Water balance in snowmelt season*

Water balance during entire snowmelt season is written as,

$$HW + P = Q + E \pm \Delta S, \tag{4}$$

where HW is snow water equivalent, P precipitation, Q discharge, E evapotranspiration, and ΔS the change in water storage under ground. The water balance period was determined from the day on which the snow water equivalent of the entire watershed was measured to the day on which the diurnal fluctuation in discharge disappeared. Table 1 shows the results. To obtain the snow water equivalents in the entire watershed, the distributions of them (Figure 4) were considered. In this watershed, the snow water equivalent was nearly constant under 400 m a.s.l., and over this height it increased with increases in altitude, as shown in Figure 4. The total discharges caused by snowmelt were estimated by the method in which the exponential extrapolation of recession limb was used for hydrograph separation (Motoyama et al. 1983). For example, the estimated discharge corresponds to the area

Table 1 Water balance. HW : snow water equivalent. P : precipitation. Q : total amount of runoff. The values in brackets are the estimated amounts discharged after the period.

Period	HW mm	P mm	Q mm	$Q/(HW+P)$
Apr. 8 – May 12, 1989	558	51	424 (12)	0.70
Mar. 30 – May 11, 1990	524	45	437 (8)	0.77
Apr. 10 – May 7, 1991	397	104	377 (14)	0.75
Apr. 6 – May 21, 1992	545	112	511 (10)	0.78

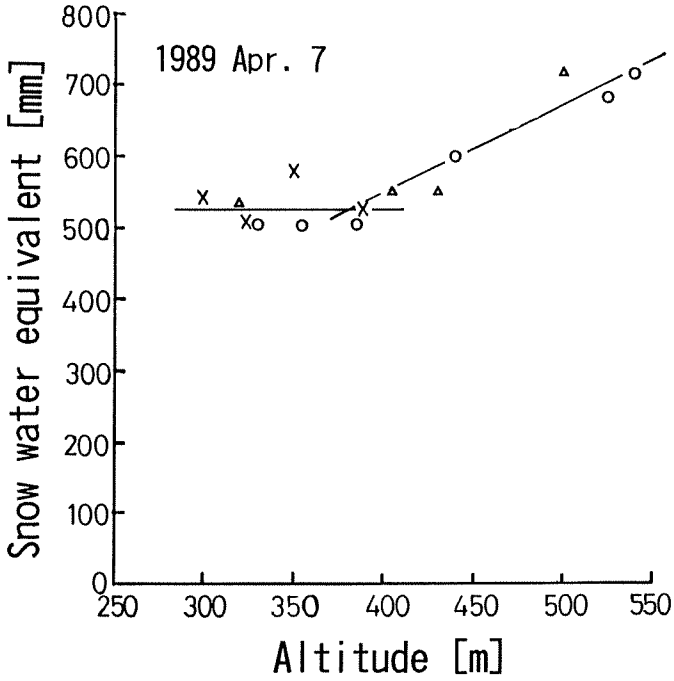

Figure 4 Altitudinal distribution of snow water equivalent. Circles : east ridge. Triangles : west ridge. Crosses : valley.

enclosed by solid and broken lines in Figure 5. The discharges estimated through the above method include the amounts discharged after the periods, however, they are caused by snowmelt. They are shown in the brackets in Table 1. The runoff coefficients ($Q/(HW+P)$) ranged from 0.7 to 0.8. Evapotranspiration in snowmelt season is very little in comparison with other components (Motoyama et al. 1983). The runoff coefficients vary within a small range and represent the character of this watershed in snowmelt season. In other

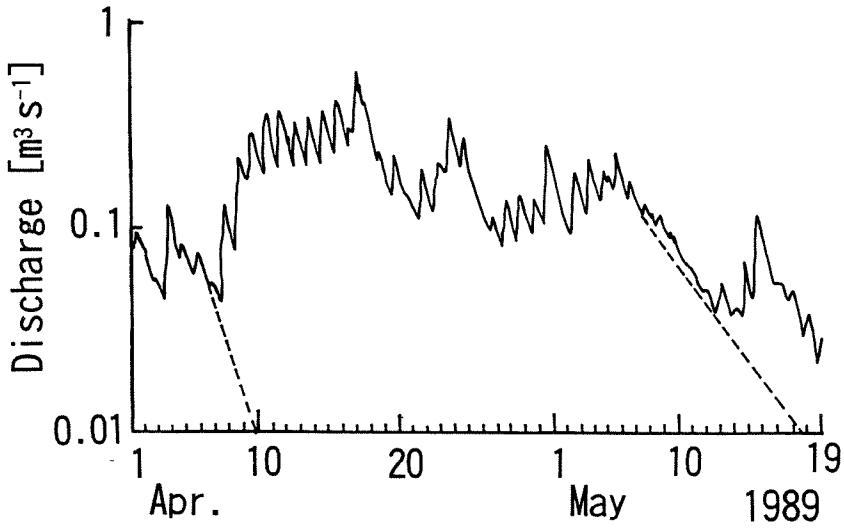

Figure 5 Runoff hydrograph during snowmelt season. Discharge is presented in logarithmic scale. Broken lines are the exponential extrapolation of recession limbs.

words, from 20 % to 30 % of meltwater is stored as groundwater recharge or lost to the neighboring watershed, assuming no storage in the snowpack. In the next section, water balance during a short period is discussed using the runoff coefficients obtained in this section.

2) *Water balance in a short period*

Water balance in one or a few days is written as,

$$M + P = Q + E \pm \Delta S_s \pm \Delta S, \tag{5}$$

where M is snowmelt, ΔS_s the change in water storage in the snowpack, and the others are the same as equation (4). The difference between equation (4) and (5) is the term ΔS_s. If the runoff coefficient ($Q/(P+M)$) for the short period is close to that for the entire snowmelt period, it could be assumed that $\Delta S_s = 0$ for the short period. Figure 6 shows that the short period runoff coefficient is very close to that of the whole snowmelt period. It is concluded that the change in meltwater storage could be ignored during the active snowmelt season.

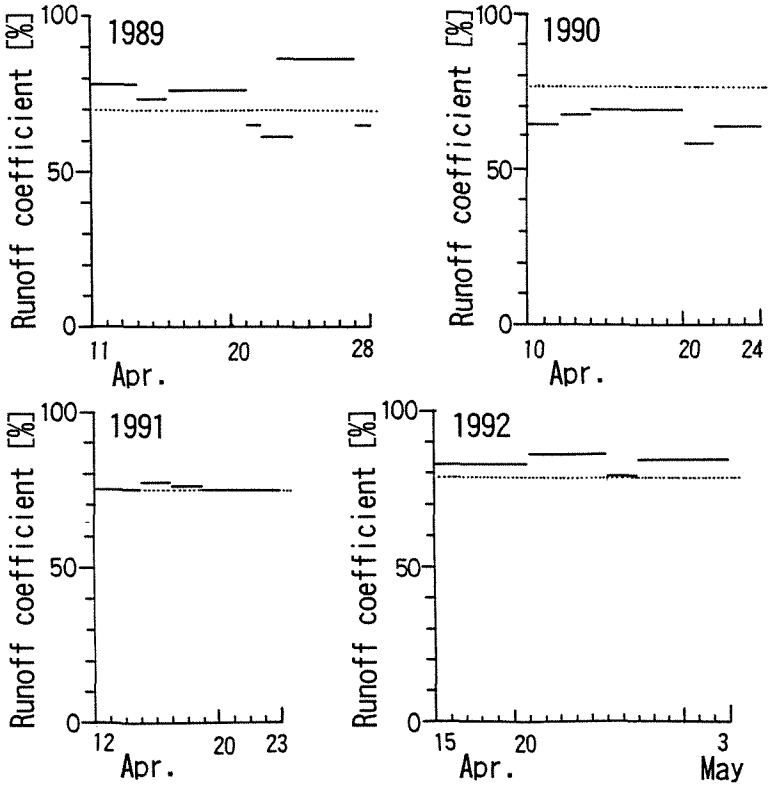

Figure 6 Runoff coefficients during snowmelt seasons. Solid lines indicate the runoff coefficients for the short period. Dotted lines indicate the runoff coefficients for the entire snowmelt periods.

2. *Delay of peak runoff*

The stream hydrograph on fine days shows a clear diurnal fluctuation with the minimum before noon and the maximum in evening, as shown in Figure 7. The delay of runoff to snowmelt was examined using the lag time from the peak snowmelt to the peak runoff. Figure 8 shows the time of peak discharge at the outlet of the watershed against snow depth at the base station. The peak time appears earlier as snow depth decreases. However, its relation is not clear for snow depth under 40 cm. It is also interesting that the peak time is different yearly for the same snow depth. For example, when snow depth was 100 cm, the peak time in 1989 was at about 17 h, while in 1992 it was at about 19 h.

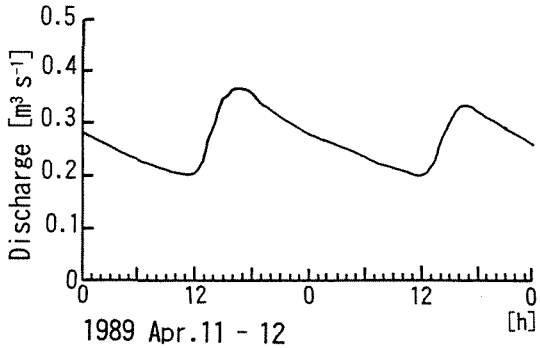

Figure 7 Runoff hydrograph of the outlet of the watershed on fine days.

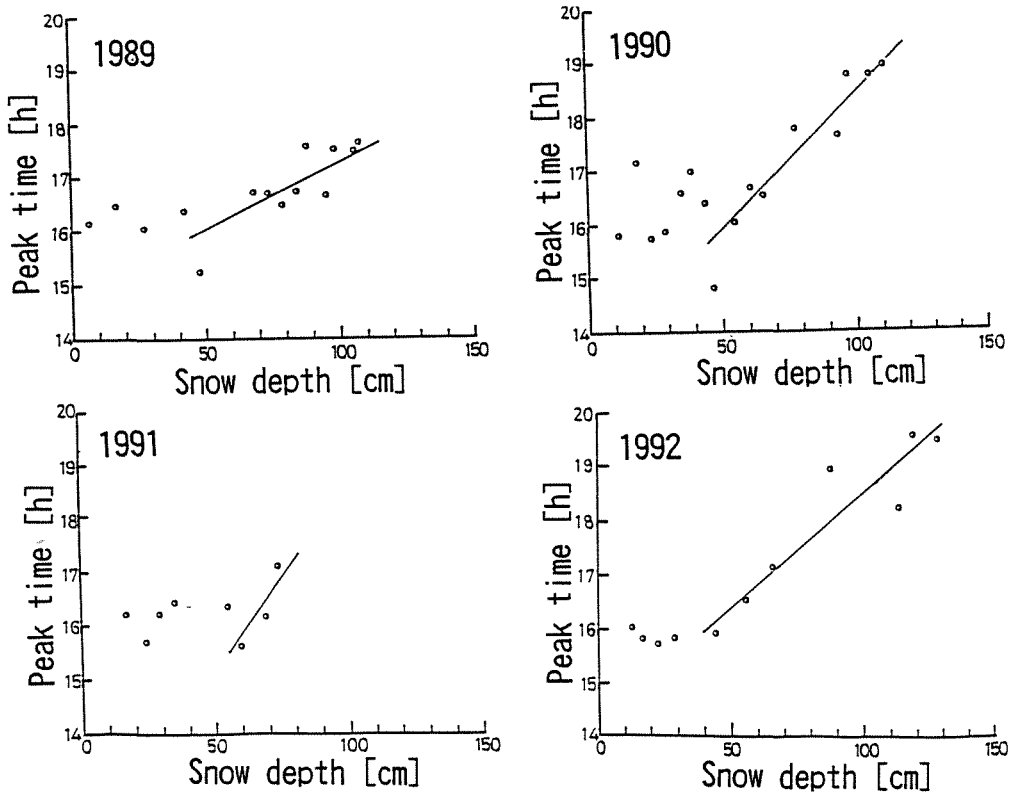

Figure 8 The relationship between the time of peak runoff at the outlet of the watershed and the snow depth at the base station.

The yearly difference in the peak time must be caused by the difference in meltwater travel time through the snowpack and soil. The travel time of meltwater from the bottom of the snowpack to the river was investigated at first. Figure 9 compares the peak time of discharge in the river to that at the bottom of the snowpack. The latter was obtained through observation with the large lysimeter installed at the base station. The broken line in each figure, which indicates a lag of 3.2 h, can represent the lag of each year. The travel

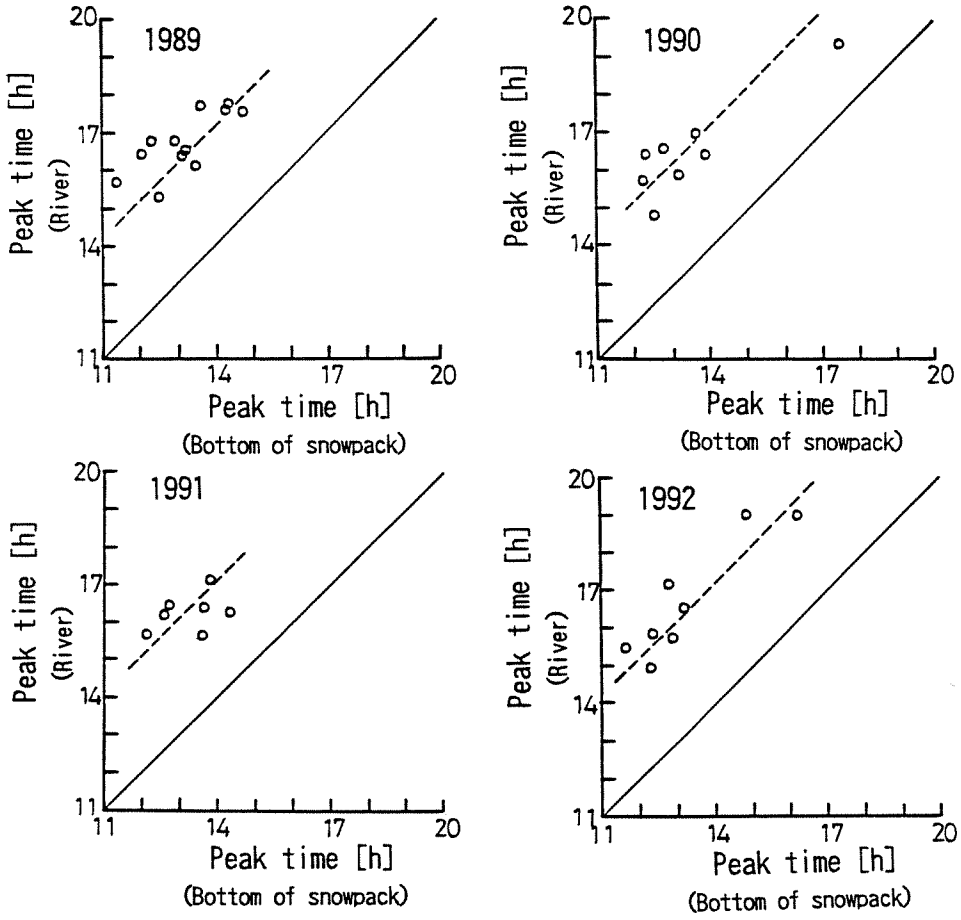

Figure 9 Time lag between the time of peak runoff at the outlet of the watershed and of the discharge at the bottom of a snowpack at the base station. Solid lines indicate the zero time lag. Broken lines indicate a time lag of 3.2 hours.

time from the bottom of the snowpack to the river is the same every year. That suggests that the runoff process in soil does not change yearly, and indicates that the yearly difference in peak time is caused by the difference in the travel time through the snowpack. It is easily guessed that the stratification in the snowpack differs yearly while the soil condition does not change. This difference in the snowpack may influence the condition of the infiltration in the snowpack and the travel time.

This chapter is summarized as follows. First, meltwater discharges into river without storage in the snowpack over the whole period in the active snowmelt season. Second, the peak time in discharge changes owing to the difference in the travel time of the infiltration through the snowpack.

IV. Meltwater infiltration through snowpack

The travel time of the meltwater infiltration through the snowpack differs yearly, as described in the previous chapter. In this chapter, the yearly difference in the speed of meltwater infiltration is investigated for the snowpacks on flat sites at the base and the top stations. The relationship between the infiltration speed and the stratification in the snowpack is discussed, and an infiltration model is developed.

1. *Travel time of meltwater infiltration through a snowpack*

1) *Method*

The snowmelt rate was estimated through the heat balance method and the discharge at the bottom of the snowpack was measured with the large lysimeters (L.L.). Though the daily discharge should be equal to the daily snowmelt during the active snowmelt season, L.L. may not measure correct discharge due to non-uniform infiltration. Then the daily discharges at the bottom of the snowpack were compared with the daily snowmelts (Figure 10). The daily discharges at the bottom of the snowpack were estimated by a method using hydrograph separation according to the exponential extrapolation of recession limb (Hamada et al. 1988). Figure 10 shows that the discharges equal the snowmelts at the base station, but the agreement is not very close at the top station. However, they are acceptable measurements because the errors in the snowmelts estimated through the heat balance method are similar.

Figure 11 shows one example of the time series of the snowmelt at snow surface and the discharge at the bottom (upper figure) and those integrated with time (lower figure). In order to investigate the time lag between snowmelt and discharge, the lags of peak and also the 'center of time' were used. The center of time was defined as the time at which half of the daily snowmelt or discharge occurs. The peak time nearly agrees with the center of time

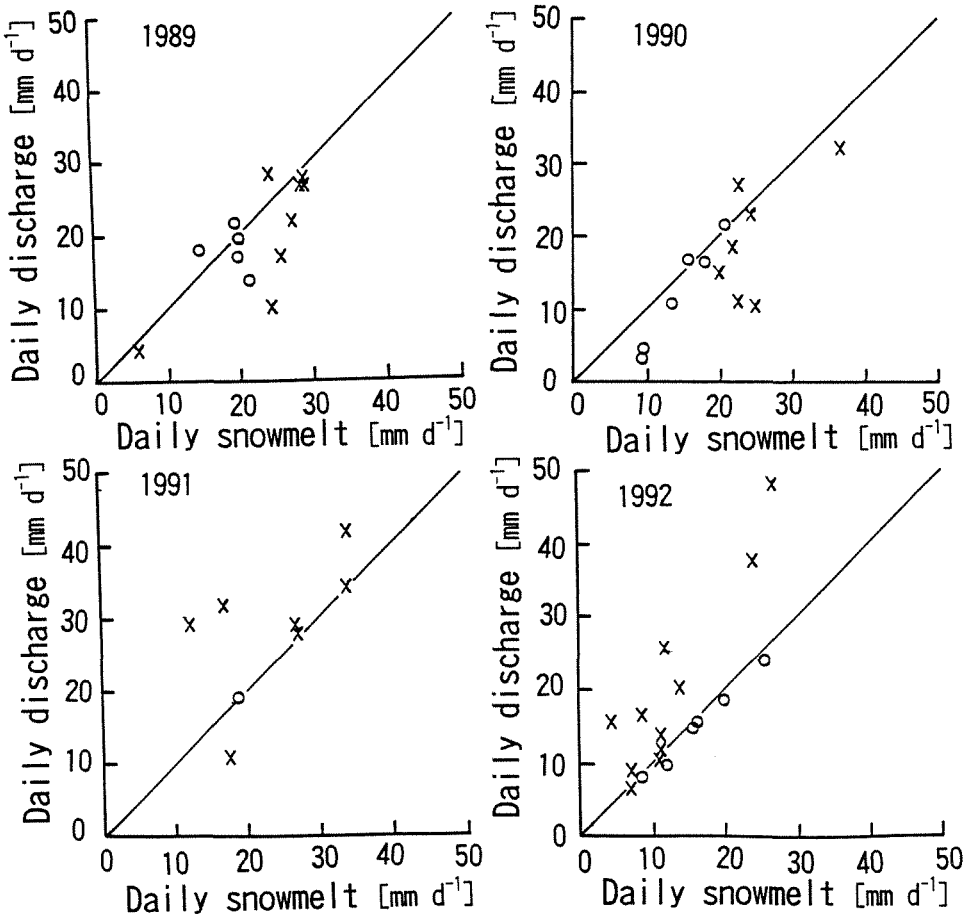

Figure 10 Comparison of daily discharge at the bottom of a snowpack with daily snowmelt. Circles : base station. Crosses : top station.

in the case of snowmelt, while the integrated discharge until the peak time is usually a few ten percent of the daily discharge, as shown in Figure 11. It is considered that the time lag between each center of time represents the average lag. In the later discussion, apparent speed, which is snow depth divided by the time lags of the center of time and peak time, is used because the snow depth is different from day to day.

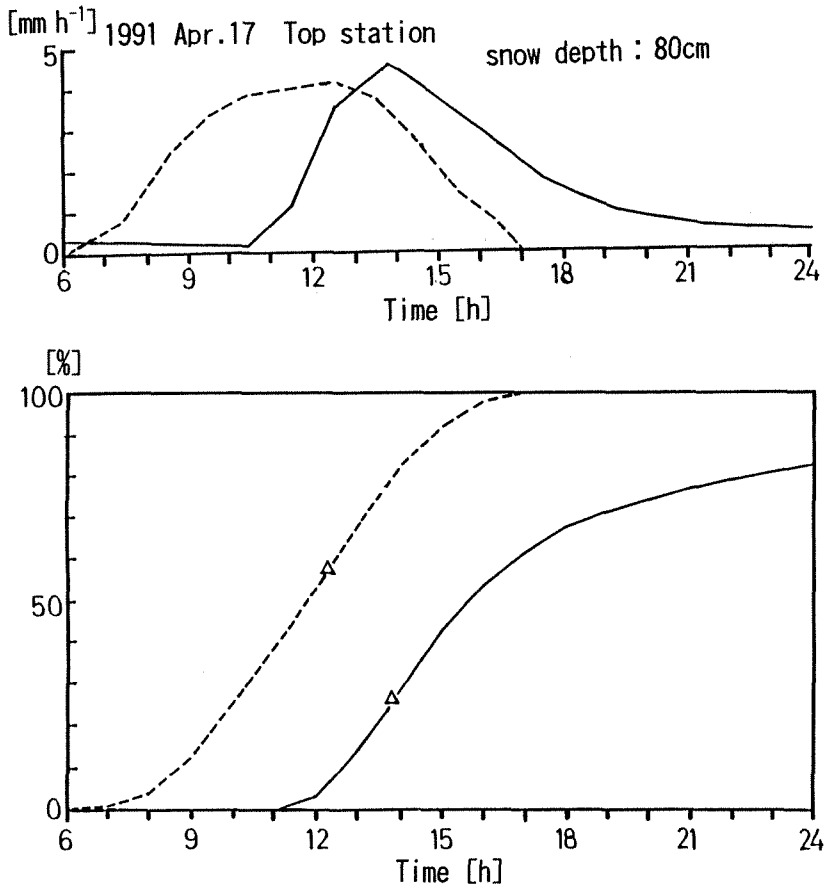

Figure 11 Time variations in snowmelt at the surface of a snowpack and discharge at the bottom of a snowpack (upper figure), and those integrated (lower figure). Broken lines indicate the snowmelt. Solid lines indicate the discharge. Triangles indicate the peak.

2) *Apparent speed of meltwater infiltration*

Figure 12 shows the speed of meltwater infiltration obtained through peak time against the peak discharge at the bottom of the snowpack. The speed tended to increase with increasing peak discharge, and the range was from 10 cm h^{-1} to 70 cm h^{-1}. The speed in 1989, in which the time of peak discharge in the river was earlier than the other years (Figure 8 in chapter III-2), was obviously the highest of all years.

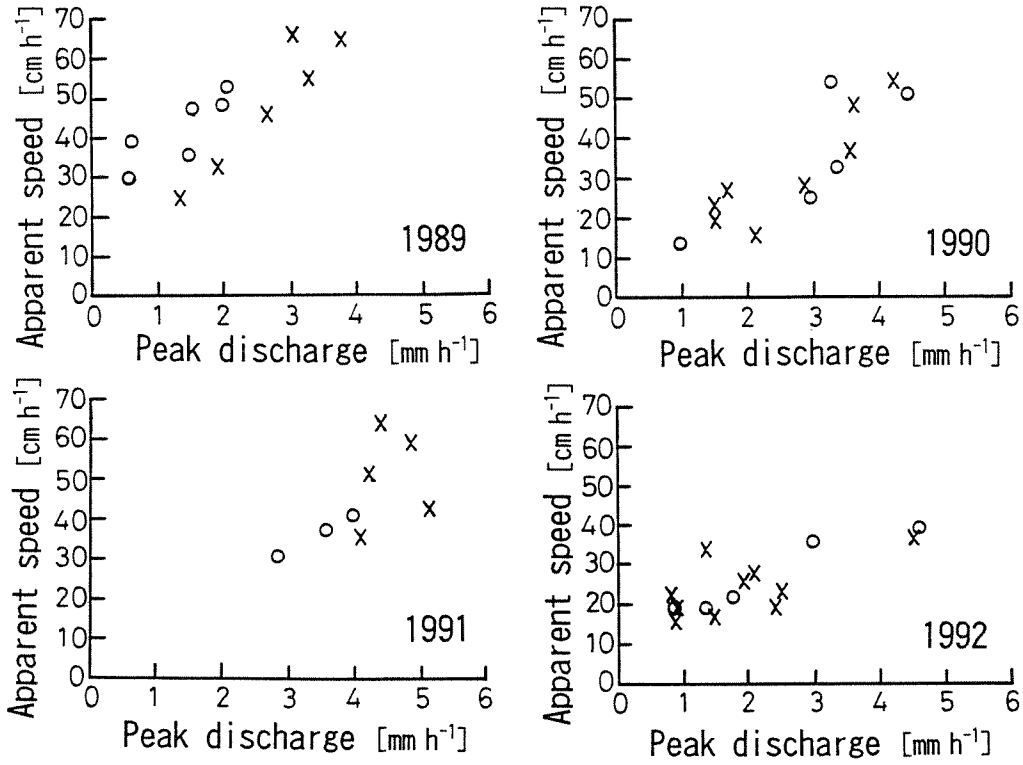

Figure 12 Relationship between the apparent speed of infiltration and the peak discharge at the bottom of a snowpack. The apparent speed of infiltration is estimated by the snow depth divided by the time lag between the peak snowmelt and peak discharge. Circles : base station. Crosses : top station.

Figure 13 shows the speed obtained by the center of time. The speed ranged from several cm h^{-1} to 40 cm h^{-1} and it was smaller than the result obtained through peak time. The tendency of the speed to increase with the increase of discharge was seen, which is consistent with the result obtained in Figure 12. The yearly difference in the speed was seen

clearly, and the difference between the highest and the lowest speed was over 10 cm h^{-1} when the daily discharge was 20 mm. The lines in Figure 13 are drawn based on Colbeck (1978)'s assumption that the propagation speed is proportional to 2/3 the power of the meltwater flux. The details of this assumption will be described in the later section. As shown in Figure 13, the lines represent the relationship between the speed and the discharge well.

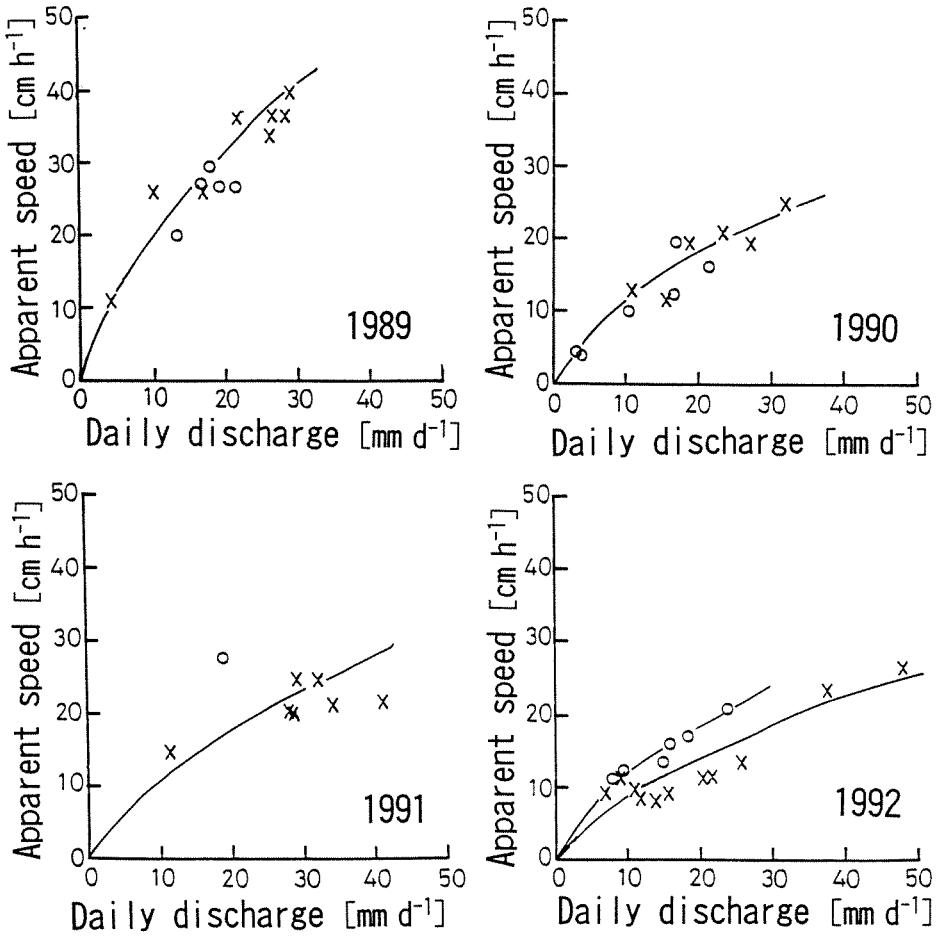

Figure 13 Relationship between the apparent speed of infiltration and the daily discharge at the bottom of a snowpack. The apparent speed of infiltration is estimated by the snow depth divided by the time lag between the centers of the integrated snowmelt and discharge. Circles : base station. Crosses : top station.

3) *Structure of a snowpack*

As described above, there was yearly difference in the speed of meltwater in the snowpack as well as yearly difference in the peak time in the river runoff. The structure of the snowpack, on which the infiltration depends, was investigated.

Figure 14 shows the results of snow pit observations at the top station. For all years, the surface and the bottom layers consisted of coarse grains, and the inner layer consisted of relatively fine grains which had not been metamorphosed much. The mean density of the snowpack was about 0.45−0.50 g cm^{-3} and it did not show a notable yearly difference. The number of ice layers in the snowpack was different yearly. The snowpack in 1989, in which the speed was large, had five ice layers, while the other years there were only one or two ice layers. Therefore, the increase of the meltwater infiltration speed could be caused by the existence of ice layers.

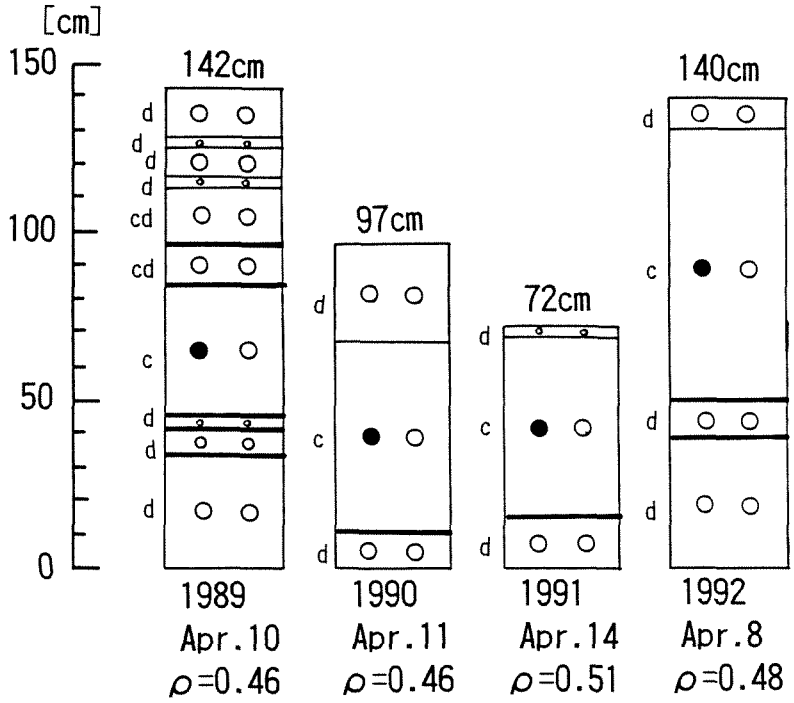

Figure 14 Stratification in a snowpack at the top station. Solid circles : compact snow. Open circles : coarse grained snow. Thick solid lines are ice layers. 'c' indicates the grain size of 1.0−2.0 mm. 'd' indicates the grain size of >2.0mm. 'cd' indicates the grains consisting of 'c' and 'd'. ρ is the mean density (g cm^{-3}) of snowpack.

2. *Infiltration process*

1) *Water-film flow and water-channel flow*

Yosida (1965) proposed two types of meltwater infiltration in the snowpack, one called 'water-film flow' and the other 'water-channel flow.' The water-film flow is the flow in a form of thin film at the surface of the snow grains, and the water-channel flow is the flow filling the gap between the grains. According to Yosida (1965), their theoretical speeds were 10^{-3} cm s^{-1} for the water-film flow and 1 cm s^{-1} for the water-channel flow. The observed speeds (Wakahama 1968, Fujino 1968) were between the above values. The actual infiltration in the snowpack must be a mixture of both types.

The water-channel flow may be dominant on days of intensive snowmelt when the speed is high. That can partially explain the relationship between the speed and the daily discharge in Figure 12 or 13. However, the problem of the yearly difference in the infiltration speed is left unsolved, because there is no yearly difference in snow grain size and density, which regulate the 'water-film' or 'water-channel' flows. The concept is not enough to describe the yearly difference in the infiltration speed.

2) *Gravity flow*

Colbeck (1978) proposed a gravity flow theory in which the infiltration in the snowpack was driven only by gravity and the gradient of capillary pressure was relatively small. This concept yields the relationship in which the propagation speed of meltwater is proportional to 2/3 the power of the flux. As shown in Figure 13, this relationship is consistent with the observational results. The proportional coefficient in this theory is determined by the grain size and the density of snow. However, the coefficient obtained by the observations differed yearly in spite of the similar grain size and density every year. That means that gravity flow alone can not explain the yearly difference in the infiltration speed. The yearly difference noticeable in the snowpack is due to the number of ice layers. The effects of ice layers on the meltwater infiltration will be discussed in the next section.

3) *Change of meltwater movement at ice layer*

The structure or mechanism of an ice layer in a snowpack has not been understood well. According to a snow pit observation, the ice layer was composed of coarse grains, which are bonded well, and the thickness was several millimeters. The ice layer is not an impermeable plate, but is rather porous.

The effects of ice layers on the meltwater movement in the snowpack were investigated with a tracer test, in which the movement of dyed meltwater was observed. The test was conducted at the flat site near the top station on May 7, 1992.

Figure 15 shows one example of dyed meltwater movement. The snowpack had two ice layers. As shown in figure, the colored meltwater moved horizontally on the ice layer, and

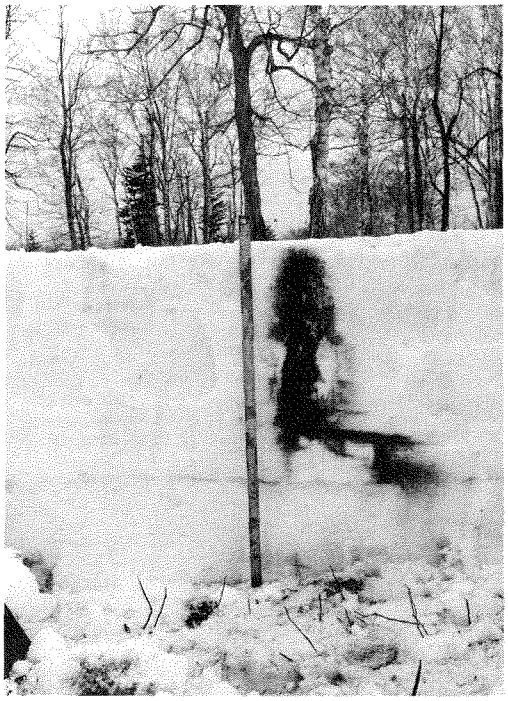

Figure 15 Photograph of dyed meltwater infiltration in a snowpack at the top station on May 7, 1992. The snow depth was 97 cm. There were two ice layers at 50 cm and 38 cm above the bottom.

then downward movement occurred again at a different point from that where the colored meltwater reached the ice layer. In such a manner, the ice layer changed meltwater movement from uniform flow to non-uniform flow.

4) *Concentrated flow*

The apparent speed of the infiltration in the snowpack with many ice layers was larger according to observational results (chapter IV-1), while an ice layer tends to cause non-uniform meltwater flow, as seen in the tracer test. The mechanism of the ice layer for meltwater movement is considered as follows.

(1) The downward movement of meltwater ceases at the ice layer.

(2) Meltwater moves on the ice layer collecting meltwater which arrived at other points.

(3) The downward movement occurs again at a point where the ice layer is relatively porous as the larger flux of meltwater than the flux above the ice layer.

If the larger flux propagates with a larger speed, the meltwater consequently arrives at the bottom of the snowpack earlier. We call the meltwater movement 'concentrated flow.'

The existence of the concentrated flow has been known (e.g. Wakahama et al. 1968), and Colbeck (1979) and Furbish (1988) pointed out the possibility of the concentration of meltwater at an ice layer. However, the effect of such a flow on the travel time in the snowpack has not been well understood. This study treats the concentrated flow as an important process which controls the travel time, and aims to develop an infiltration model which includes this process. The development of the model depends on observation in this study.

3. *Observation of concentrated flow*

1) *Method*

The non-uniformity of meltwater flows in the snowpack was observed with a multi-compartment lysimeter (Figure 16) at the base station. A similar lysimeter was initially used by Marsh and Woo (1984a), but the present study used a larger lysimeter than theirs. The lysimeter was 2 m^2 (1.4 m×1.4 m) in area, divided into 100 individual compartments which collected meltwater into bottles. We called this lysimeter M.C.L.. The lysimeter was installed at the level of the ground surface from the inside of an underground trench just before the snowmelt season. The trench was dug before the snowy season, and had been covered with a board in order to accumulate snow naturally. The observations were made for one day in 1991 and for four days in 1992.

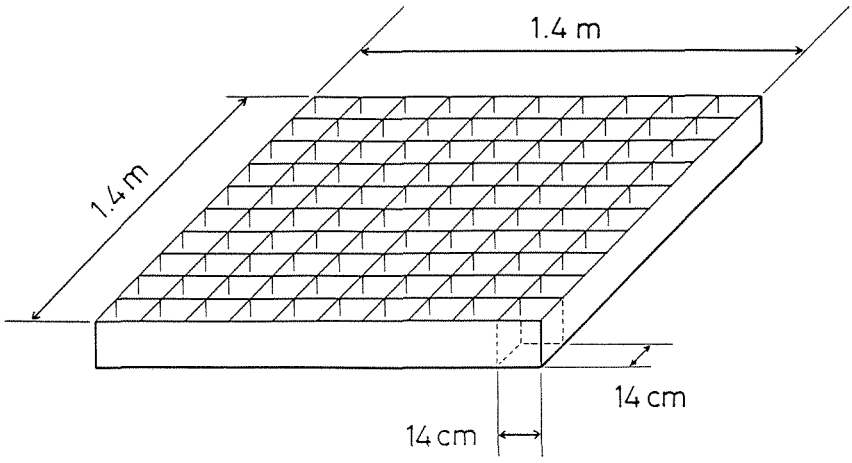

Figure 16 Schematic diagram of the multi-compartment lysimeter.

2) *Results*

Figure 17 shows the observed distribution of the discharges at the bottom of the snowpack. The discharges were classified in four groups depending on the intensity of concentration, which was defined as the daily discharge divided by the daily snowmelt. As shown in Figure 17, concentrated flows existed, and the position did not change much in the period. In other words, there were fixed flow paths of meltwater in the snowpack.

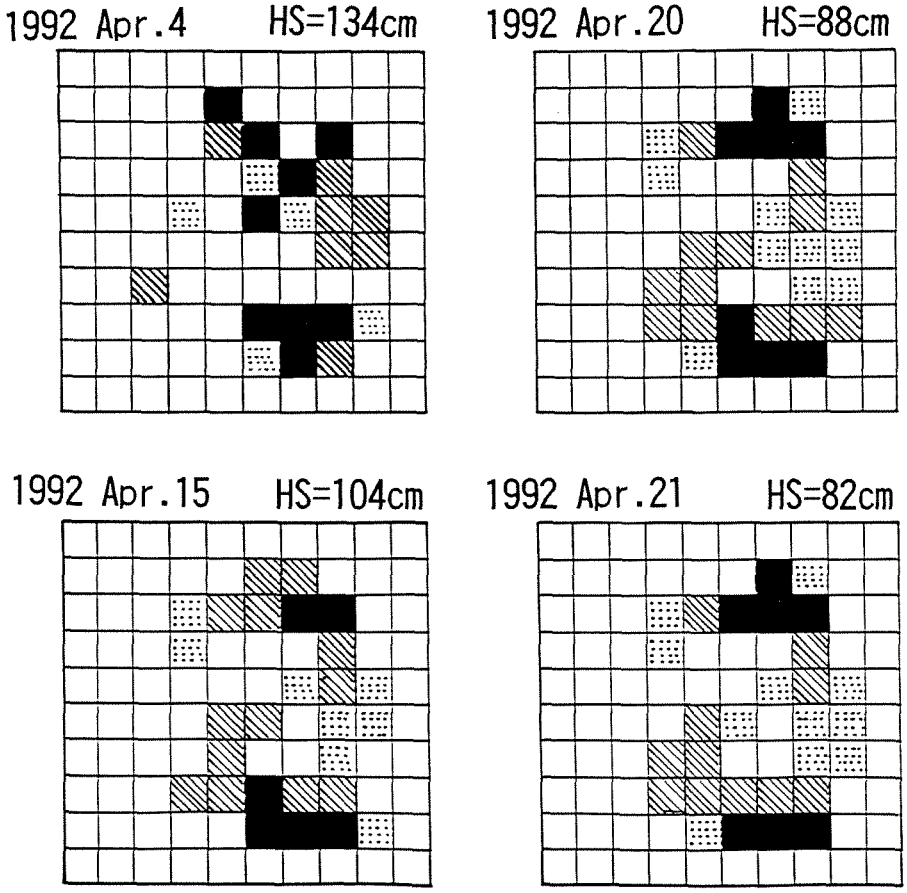

Figure 17 Distribution of discharges at the bottom of a snowpack. These are classified by the intensity of concentration. The intensity is defined as the daily discharge of the compartment divided by daily snowmelt. Solid : the intensity of >10. Oblique : the intensity of $2-10$. Dotted : the intensity of $1-2$. Open : the intensity of <1. HS indicates the thickness of snowpack.

Figure 18 shows the number of compartments for the intensity of concentration. High concentrations were seen above the concentration intensities of 20, but the number of such high concentrations was small. The number of concentrated flows of which the intensity was larger than about 10 decreased notably.

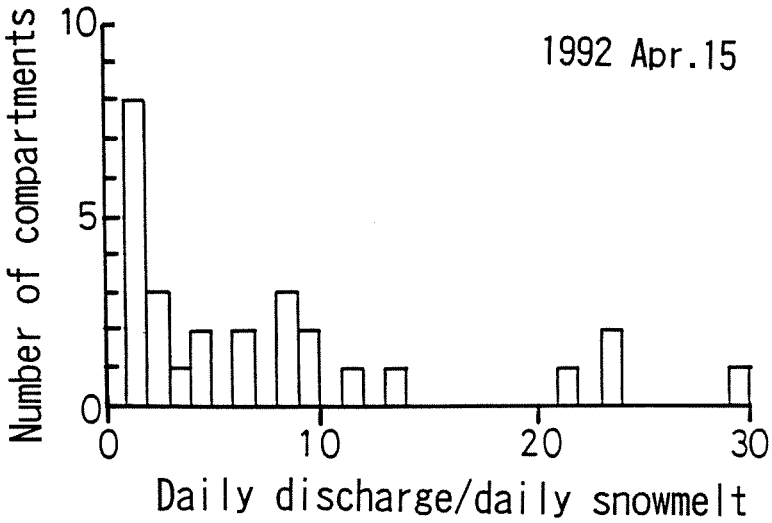

Figure 18 The numbers of compartments against the intensity of concentration (daily discharge/daily snowmelt).

In the previous section, we assumed that the propagation speed of meltwater increased when the meltwater flows were concentrated. Here the speed of the concentrated flow was investigated using the apparent speed estimated through 'center of time' (defined in chapter IV-1). First, the speed obtained with the total discharge of the multi-compartment lysimeter (M.C.L.) was compared with that obtained with the large lysimeter (L.L.) (Table 2). The total daily discharges measured with M.C.L. were about 1.5 times as much as the daily snowmelt in 1991 and about 2.5 times as that in 1992, whereas those measured with L.L. were equal. The speed obtained by M.C.L. was larger than that by L.L.. This difference could probably be caused by the difference in the concentration intensity between the two lysimeters.

Further more, the infiltration speed obtained through each compartment of M.C.L. was investigated. Figure 19 shows the speeds compared to the daily discharges in the compartments in which the discharge yields were not less than twice the snowmelt rates. No clear relationships between those are seen, which is different from the results of L.L. (Figure 13).

Table 2 Comparison between the results observed with the multi-compartment lysimeter (M. C. L.) and with the large lysimeter (L. L.). *HS* : snow depth. *M* : daily snowmelt. *Q* : daily discharge. *V* : apparent speed of infiltration which is estimated the snow depth divided by the time lag between the center of the integrated snowmelt and discharge.

Date	*HS* [cm]	*M* [mm/d]	M. C. L. *Q*[mm/d]	M. C. L. *V*[cm/h]	L. L. *Q*[mm/d]	L. L. *V*[cm/h]
1991 4/12	55	19.1	29.6	35.6	19.0	27.4
1992 4/ 4	134	18.0	36.1	20.6	no observation	
1992 4/15	104	19.9	43.1	29.5	19.9	17.0
1992 4/20	87	16.3	45.0	24.2	18.0	16.1
1992 4/21	82	25.6	63.7	32.3	27.1	21.1

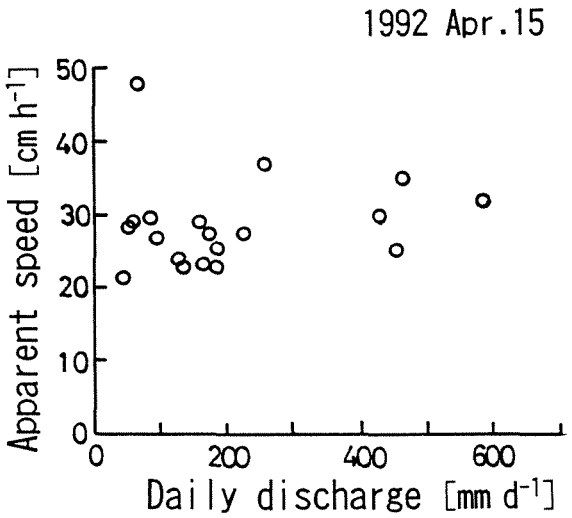

Figure 19 The relationship between the apparent speed of concentrated flow and the daily discharge obtained by each compartment of M.C.L. of the daily discharge/the daily snowmelt ≧2.

For some compartments, the speed of the low concentrated flow was larger than that of the high concentrated flow. The reason may be the difference in the level at which meltwater concentrates. There were two ice layers in the snowpack at this observation (Figure 20). The flow concentrated at the upper ice layer may arrive at the bottom earlier than that concentrated at the lower ice layer when the concentration intensities of both flows are equal. Thus, the apparent speed of the high concentrated flow is not always larger than that of the lower one.

The reality of concentrated flow is very complex, as described above. The results were arranged in order to develop a model. This arrangement was made without the data of April 4, 1992, in which the structure of the snowpack was not known. Because the number of concentrated flows of which the intensity was larger than 10 was notably small, the

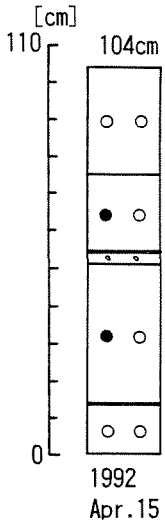

Figure 20 The stratification of the snowpack at base station on April 15, 1992. Solid circles : compact snow. Open circles : coarse grained snow. Thick solid lines are the ice layers.

concentrated flows were classified in two types, depending on the intensity of concentration. A type of concentration intensity over 10 is called 'high concentration,' and that under 10 is called 'low concentration.' Table 3-(1) shows the rate of the numbers of each type and the rate of amounts discharged by each type. For the development of a model, Table 3-(1) is summarized as Table 3-(2). Here the point to which attention should be paid is that there must be non-concentrated flows in the snowpack which are not presented in Table 3. This flow is considered in the next section.

Table 3 Results of concentrated flows. (1) The observational results. 'High' indicates the intensities of concentrations more than 10. 'Low' indicates the intensities of concentrations between 2 and 10. (2) is a summary of (1).

(1)

Date	Number of compartments		Percentage of the discharges	
	High	Low	High	Low
1991 4/12	5	9	71	29
1992 4/15	6	13	61	39
1992 4/20	8	12	73	27
1992 4/21	7	11	70	30

(2)

	Intensity	Ratio of numbers	Ratio of discharges
High concentration	> 10	2	7
Low concentration	2 - 10	3	3

4. *Infiltration model*

1) *Pattern of meltwater flows*

On the basis of the above results, three types of flows in the snowpack were assumed in the model. Those were 'high concentration,' 'low concentration' and 'non-concentration.' The characteristics of the concentration types were determined with the observational results described in the previous section, and those of the non-concentration type were determined by the structure of the ice layer at which meltwater concentration occurs.

The observations of the concentrated flows were made for the snowpack which had two ice layers. Then the intensity and the number of concentrated flows were determined, as shown in Table 4, for the case of two ice layers. The procedure of the determination is as follows. The ratio of the number of each type is given in Table 3-(2). The intensities of high and low concentration are given as 10 and 3 because these values and the ratio of numbers of each type determined above yields the ratio of the amounts discharged for each type as closely as that observed.

Table 4 Assumed concentrated flows.

	Intensity	Ratio of numbers	Ratio of discharges
High concentration	10	2	6.7
Low concentration	3	3	3

The characteristics of each type are assumed as follows. The high concentration type is a meltwater flow which concentrates once at an ice layer. For the snowpack with two ice layers, there are two patterns of high concentrated flows, which concentrate at the upper ice layer and at the lower ice layer. The low concentration type is a meltwater flow concentrating at every ice layer. The intensity of this flow increases by 1 at every concentration so that the intensity for the snowpack with two ice layers becomes 3, as shown in Table 4.

For the complete pattern of flows, we must determine the ratio of the number of non-concentrated flows to concentrated flows. For this purpose, the structure of the ice layer is considered. As described in chapter IV-2, the ice layer in the snowpack is composed of coarse grains and it is not an impermeable plate. This study shows that an ice layer is formed of permeable and impermeable parts (Figure 21). For the concentration, the impermeable ice layer must prevent downward movement of meltwater and promote lateral movement on it by gathering the meltwater. In the permeable area, the meltwater passes through without concentration. If the ratio of both areas is known, the number of non-concentration flows must be determined. The ratio is estimated as follows. The density of the entire ice layer is assumed to be 0.55 g cm^{-3}, which is the extreme value measured by snow pit observations. The density of the permeable area is assumed to be 0.50 g cm^{-3} of

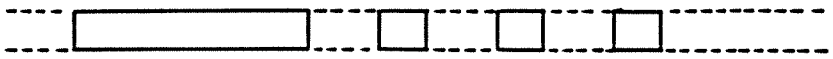

Figure 21 Assumed ice layer. The parts of solid lines indicate impermeable areas, and the parts of broken lines indicate permeable areas.

the usually observed maximum density. The density of the impermeable area is assumed to be 0.80 g cm^{-3} because snow becomes impermeable at about that density (Maeno and Fukuda 1986). 1 : 5 is obtained as the ratio of the impermeable to the permeable area in order to match the ice layer density of 0.55 g cm^{-3} with the permeable area density of 0.50 g cm^{-3} and the impermeable area density of 0.80 g cm^{-3}. The high concentration intensity of 10 needs an impermeable area of 9 and a permeable area of 1. In the case of the low concentration intensity of 2, the impermeable area is 1 and the permeable area is 1. In order to explain the ratio of the number of high and low concentration types shown in Table 4, we assumed the pattern of meltwater flows in the snowpack with two ice layers as shown in Figure 22. For an ice layer, the impermeable area should have an area unit of 12, which consists of 9 area units for high concentrations and 3 for low concentrations. At the permeable area of 60 area units, which is five times as large as impermeable area, meltwater passes through an ice layer. Meltwater infiltrates uniformly above the first ice layer. Concentrations occur at the ice layer, so the number of non-concentration flows decreases in accordance with the number and the intensities of the concentrations. This study regards that all ice layers have the same structure, and that the same manner occurs at every ice layer.

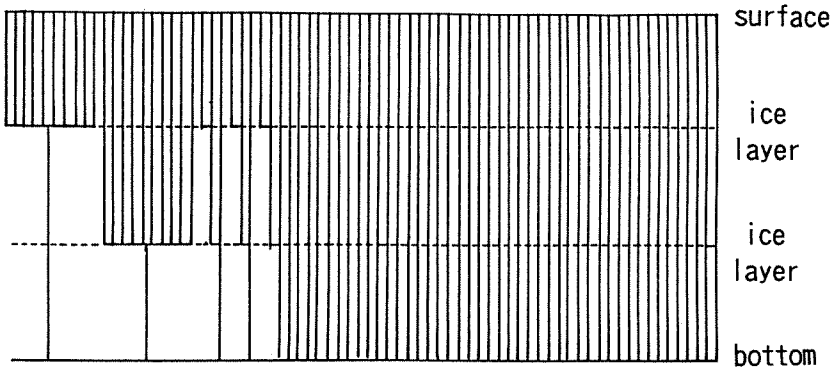

Figure 22 Assumed meltwater flows in a snowpack with two ice layers.

2) *Method of calculation*

This section describes the calculation method of the infiltration through the snowpack for the simulation of the discharge at the bottom of the snowpack. The present study used the kinematic wave method developed by Colbeck (1978).

Darcy's equation extended in an unsaturated zone is

$$q = -K\left(\frac{\partial \psi}{\partial z} - 1\right), \tag{6}$$

where q is the meltwater flux, K the unsaturated hydraulic conductivity, ψ the capillary pressure head, and z the depth from snow surface. The gradient of capillary pressure is assumed to be negligibly small, and the equation (6) is simplified to

$$q = K. \tag{7}$$

The continuity equation for the water at a depth in the snowpack is

$$\phi_e \frac{\partial S^*}{\partial t} + \frac{\partial q}{\partial z} = 0, \tag{8}$$

where ϕ_e is the effective porosity, S^* the effective saturation, and t the time. According to Colbeck (1978), the unsaturated hydraulic conductivity in snowpack is described using the saturated hydraulic conductivity K_s and the effective saturation as follows.

$$K = K_s S^{*3}. \tag{9}$$

Substituting equation (9) into (7),

$$q = K_s S^{*3}. \tag{10}$$

Combining equation (10) and equation (8) gives

$$\frac{\partial q}{\partial t} + \frac{3K_s^{\frac{1}{3}}}{\phi_e} q^{\frac{2}{3}} \frac{\partial q}{\partial z} = 0. \tag{11}$$

According to the method of characteristics, equation (11) gives the following relation.

$$\left.\frac{dz}{dt}\right|_q = \frac{3K_s^{\frac{1}{3}}}{\phi_e} q^{\frac{2}{3}}. \tag{12}$$

Equation (12) shows that meltwater flux propagates at the rate of two-third powers of flux.

The above relationship between the flux and the rate may cause a situation in which slow moving fluxes in the morning are overridden by faster moving afternoon fluxes. This complex situation is overcome by Colbeck (1978). Continuity in the vicinity where the faster flux overrides the slower one is expressed as,

$$(q_+ - q_-)\Delta t = (S_+^* - S_-^*)\Delta\xi \ , \tag{13}$$

where q_+ and q_- are the faster and slower fluxes, S_+^* and S_-^* are the saturations above and under this vicinity, Δt is the infinitesimal time, and $\Delta\xi$ is the infinitesimal thickness of the vicinity. Combining equations (10) and (13) gives

$$\frac{d\xi}{dt} = K_s^{\frac{1}{3}} \phi_e^{-1}(q_+^{\frac{2}{3}} + q_+^{\frac{1}{3}} q_-^{\frac{1}{3}} + q_-^{\frac{2}{3}}). \tag{14}$$

After the arrival of a larger flux, $\Delta\xi$ propagates at the rate given in equation (14).

Saturated hydraulic conductivity K is given by

$$K_s = k\frac{g\rho_w}{\eta} \ , \tag{15}$$

where k is the intrinsic permeability, g the gravitational acceleration, ρ_w the density of water, and η the viscosity. Shimizu (1970) presented the k of snow empirically using the grain diameter d and the specific gravity of snow ρ_s^* as follows.

$$k = 0.077 d^2 \exp(-7.8\rho_s^*). \tag{16}$$

Effective porosity ϕ_e is expressed by

$$\phi_e = \phi(1 - S_{wi}), \tag{17}$$

where ϕ is the porosity and S_{wi} the irreducible water saturation. ϕ is

$$\phi = 1 - \frac{\rho_s}{\rho_i} \ , \tag{18}$$

where ρ_s and ρ_i are the densities of snow and ice respectively. The value of S_{wi} is about 0.03−0.04 (Colbeck 1978), and 0.03 was used in this calculation.

Water flux q at the snow surface is the snowmelt estimated by heat balance, and q in the snowpack is changed depending on the concentration, as shown in Figure 22.

3) *Change of discharge caused by concentration at ice layers*

The present model features the process of the concentration of meltwater at the ice layer. First, we examine how the model changes the discharge at the bottom of the snowpack by the concentration.

The calculations were made for six snowpacks of zero to five ice layers at an equal distance. The thickness of the snowpacks is fixed at 100 cm. The density and the grain diameter were 0.45 g cm^{-3} and 1.0 mm, respectively. Figure 23 shows the snowmelts and

calculated hydrographs. The calculated discharge for five ice layers in the snowpack occurred notably earlier than that for no ice layers in snowpack. Similar calculations were made for different inputs. Figure 24 shows the change in the speeds, which are estimated using center of time, with the numbers of ice layers. The speed increases with an increase in the number of ice layers. In the case of daily snowmelt of 30 mm, the speed in the snowpack with no ice layers was 26 cm h^{-1}, while the speed in the snowpack with five ice layers increased to 40 cm h^{-1}.

Next, calculations were made to assess the changes caused by different ice layer

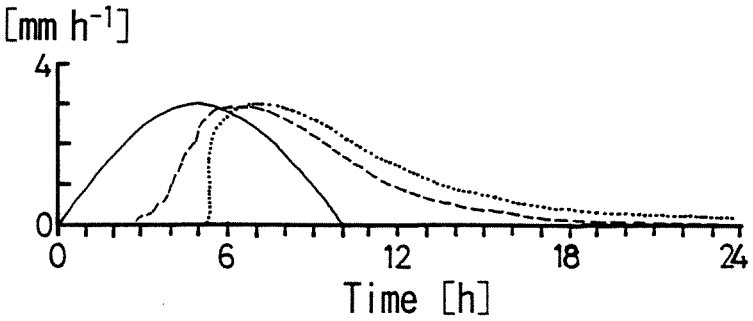

Figure 23 Calculated results of discharge at the bottom of a snowpack. The dotted line is for a snowpack without ice layer. The broken line is for a snowpack with five ice layers. The solid line is snowmelt. In this calculation, the daily snowmelt is 20 mm, and the thickness, density and grain size of the snowpack are 100 cm, 0.45 g cm^{-3} and 1.0 mm, respectively.

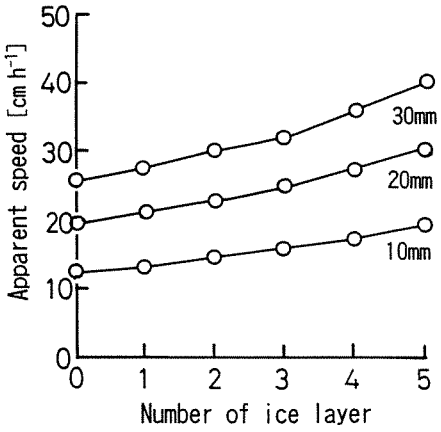

Figure 24 Relationship between the apparent speed of infiltration and the number of ice layers. The speed was estimated by the snow depth divided by the time between the center of integrated snowmelt and discharge. The values in the figure indicate the daily snowmelt.

positions in the snowpack. The calculations were done for four snowpacks of 100 cm in thickness with two ice layers, which were located at the levels of 10 cm and 20 cm, 30 cm and 40 cm, 50 cm and 60 cm, and 70 cm and 80 cm above the bottom. The density, the grain diameter, and the meltwater inputs were the same as in the previous experiment. Figure 25 and 26 show the results. When the ice layers are located at higher levels, the discharge occurs earlier because faster concentrated meltwater flow occurs in the longer path.

As shown above, the ice layers influence notably the discharge at the bottom of snowpack.

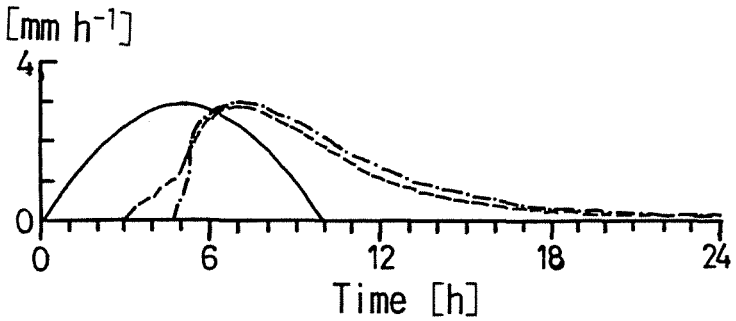

Figure 25 Calculated results of discharge at the bottom of a snowpack. The dotted dash line is for a snowpack with two ice layers located at a level of 10 cm and 20 cm above the bottom. The broken line is for a snowpack with two ice layers located at a level of 70 cm and 80 cm above the bottom. The solid line is snowmelt. The daily snowmelt amount, depth, density and grain size of the snowpack are the same as those in Figure 23.

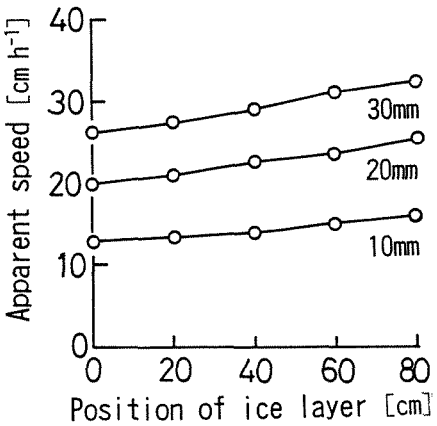

Figure 26 Relationship between and the apparent speed of infiltration and the position of ice layers. There are two ice layers at the level indicated at the abscissa and at 10cm below it. The values in the figure indicate the daily snowmelt.

4) *Simulation of observed discharge*

The observed hydrographs were simulated with this model. In this calculation, because the snowmelt estimated through the heat balance method is not always equal to the observed discharge, the snowmelt of input was adjusted to be equal to the observed discharge.

Figure 27 shows the results and the structure of the snowpack. In the case of 1989, the calculated discharge taking concentration into account occured much earlier than that assuming no concentration, and the former simulated the observed hydrograph better. In the other years, though the results of concentration and non-concentration types are not much different due to the small numbers of ice layers, the simulations are good.

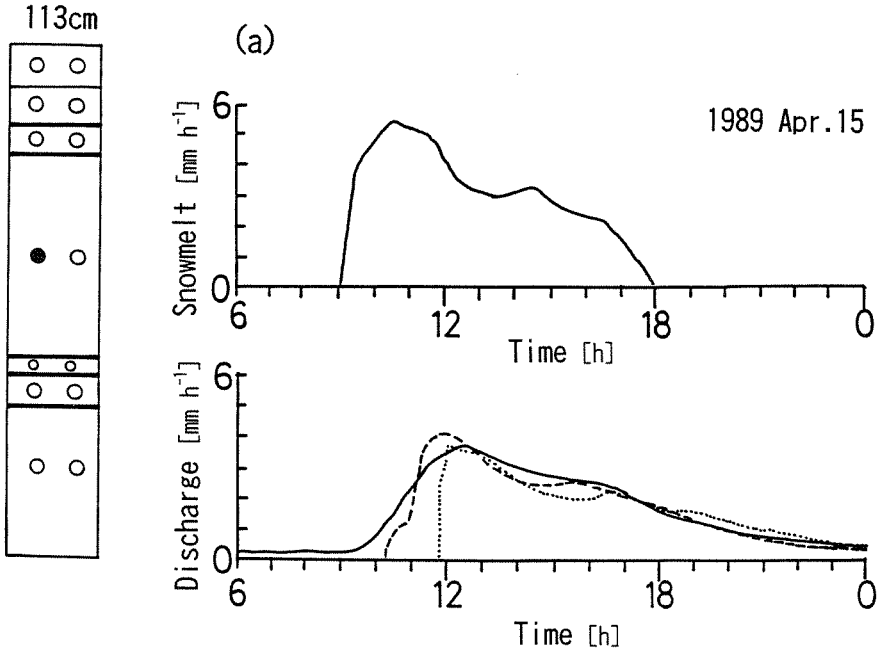

Figure 27 (a) Observed snowmelt and discharge at the bottom of a snowpack, calculated discharge, and the stratification of the snowpack. The upper figure shows the observed snowmelt. In the lower figure, the solid line is the observed discharge, the dotted line is the calculated discharge without concentrations, and the broken line is the calculated discharge with concentration. The left figure shows the stratification of the snowpack. The symboles are the same as those Figure 14. The value indicates the thickness of the snowpack.

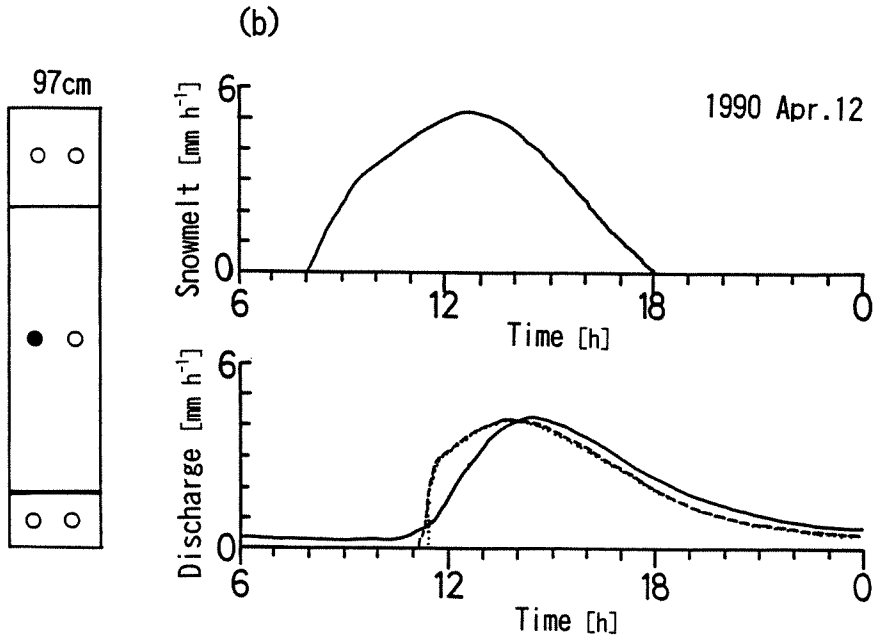

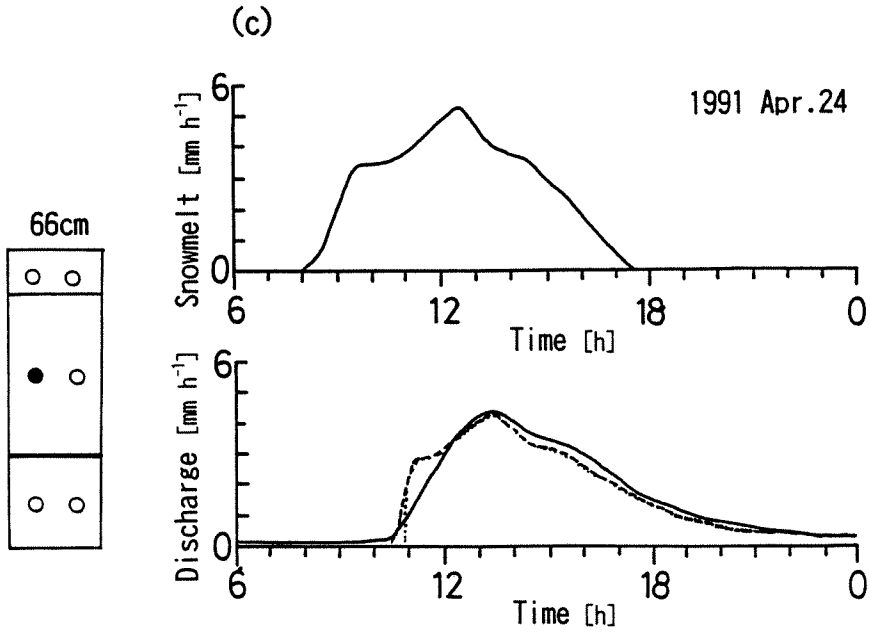

Figure 27 (b)-(c) The notations are the same as in Figure 27 (a).

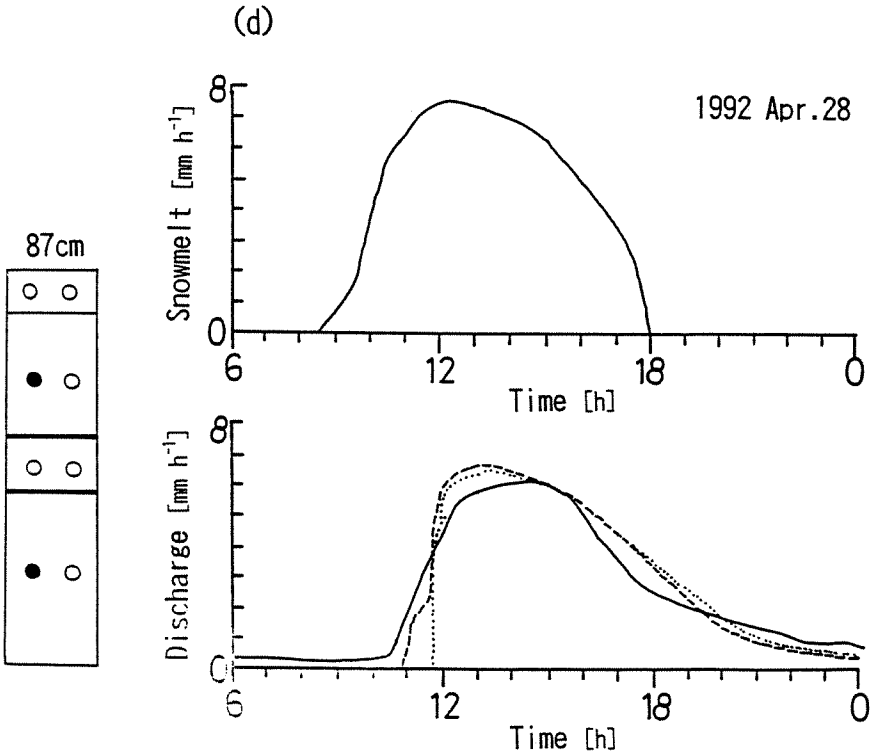

Figure 27 (d) The notations are the same as in Figure 27 (a).

Figure 28 shows the results for the late period in the snowmelt season. In this period, the observed snow depth was small and the ice layers at the upper part of the snowpack disappeared, and the number of concentration flows could have been small and the paths shortened. In these circumstances, the concentrations did not change the hydrographs much. However, the lower ice layers must have influenced the apparent speed. The speed in 1989 was the highest due to larger number of ice layers at the lower part of the snowpack.

Consequently the model can simulate the hydrographs during the active snowmelt season and present the yearly difference in the speed.

This chapter has pointed out that the apparent speed of meltwater in the snowpack with several ice layers was larger than that in the more homogeneous snowpack, and the speed differed yearly. The author considered the process of meltwater concentration at ice layers which increased the infiltration speed, and observed the concentrated flows. The model was developed on the basis of the observation, and it could reproduce the observed hydrographs and the yearly difference in the speed very well.

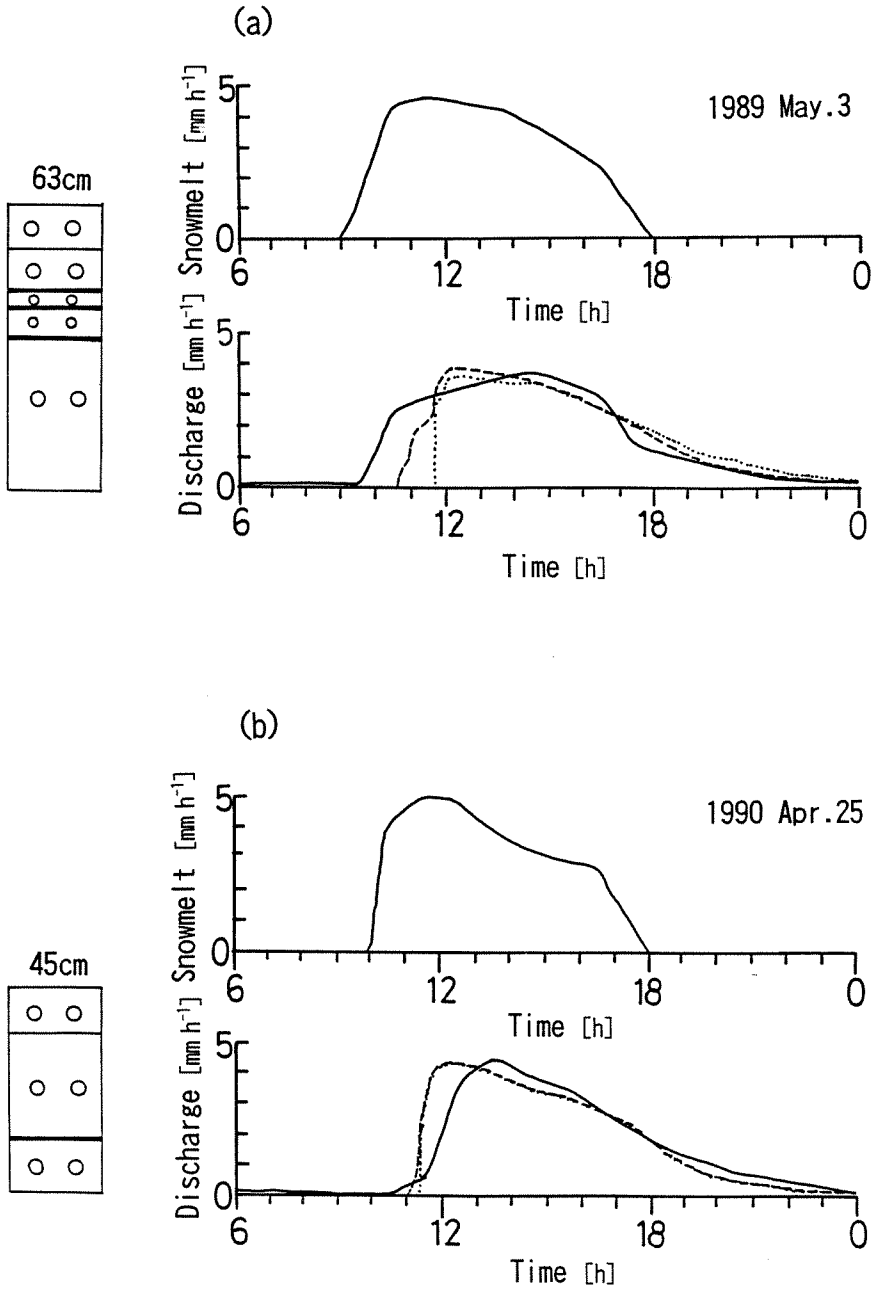

Figure 28 (a)-(b) The same as Figure 27, but for the late period in the snowmelt season.

V. Variation in infiltration through snowpack in a watershed

A watershed is not covered uniformly with snow. In order to discuss the infiltration through the snowpack as a part of the runoff process, the variation of the infiltration in the watershed should be made clear. This chapter considers two points. The first is the change caused by the difference in altitude because generally snow depth or snow water equivalent increases with altitude. The second is the infiltration through the snowpack on slopes because the greater part of a watershed consists of slopes.

1. *Comparison of the infiltration at the highest site with the lowest site of the watershed*

The meltwater infiltration through the snowpack on a flat site at the top station (TS) located at the highest part of the watershed is compared with that at the base station (BS) at the lowest part. The differences in snow depth and snow water equivalent between the two sites is maximum because they increase with altitude.

Figure 29 shows one example of the meltwater hydrographs at the bottom of the snowpack observed with the large lysimeters at the two sites. The discharge at TS was delayed due to the thicker snowpack, and the difference in the structure of the snowpack may influence the delay. The structures of the snowpacks at the two sites are shown in Figure 14 (chapter IV-1) and Figure 30. Both snowpack structures are similar. The surface and

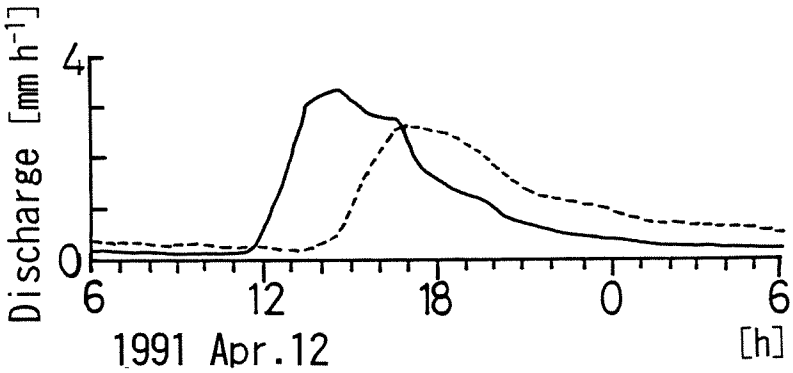

Figure 29 Observed discharges at the bottom of snowpacks at the base station (solid line) and top station (broken line). The thicknesses of the snowpacks were 56 cm at the base station and 114 cm at the top station.

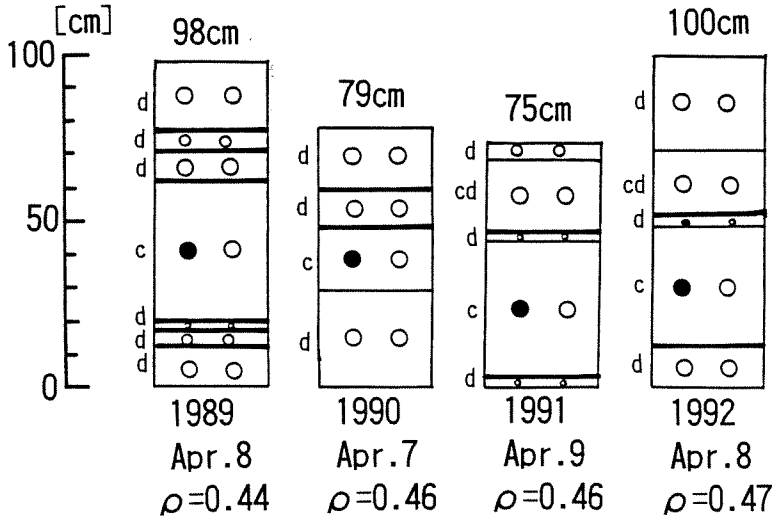

Figure 30 Stratification of snowpacks at the base station. The symbols are the same as those in Figure 14.

the bottom layers consisted of coarse grains, and the inner layers had relatively fine grains. The numbers of ice layers at both sites were nearly equal, though the positions did not always correspond with each other. These facts suggest that the infiltration speeds through the snowpacks are equal at both sites. As shown in Figure 13 (chapter IV-1), the relationships between the speed and the daily discharge at each site were presented by the same most appropriate line, except for 1992. The difference in the most appropriate lines in 1992 between the two sites was smaller than the yearly difference. Thus the travel time through the snowpack at the top site was larger than at the lowest site, being proportional to the difference in snow depths at the two sites.

There are notable differences in not only snow depth but also weather conditions in winter between the top station and the base station. However, the speeds in the snowpacks were equal at both sites. Thus, as long as the site is flat, the delay in the discharge at the bottom of the snowpack could be obtained by determining the snow depth, which can estimated for the whole watershed.

2. *Comparison of the infiltration on a slope and flat site*

The travel time through the snowpack on a slope may be delayed due to meltwater movement along slope. The tracer test examined the travel time and the path of the meltwater. This test was done by observing the movement of meltwater colored by dye. This observation was made in 1992 on a slope facing southwest at an altitude of 470 m a.s.l. (solid circle in Figure 1 in chapter II) and on a flat site near the top station to compare. The slope has an inclination of 20°.

Figure 31 shows the situation of meltwater movement in the snowpack. There were ice layers where the meltwater moved along the slope. In the other part of the snowpack, the meltwater moved vertically. Table 5 presents the results. The travel times shown in Table 5 are adjusted to correspond to the snow depth of 100 cm. The maximum length of the movement along the slope was about 200 cm. In spite of such movement, the travel times of meltwater from the surface to the bottom of the snowpack were 140 min. or 160 min., and they were close to 140 min., which was observed at the flat site. The reason for the small difference in the travel times of the meltwater in the snowpacks on the slope and the flat site could be explained by the high speed along slope. Table 6 shows the speeds of the meltwater movement along slope and vertical. Meltwater moved along slope at the rate twice or three times as high as vertical speed. This result is consistent with those observed by Wakahama (1968) and Fujino (1971).

Figure 31 Photograph of dyed meltwater in a snowpack at the slope. The snow depth was 61 cm. There were two ice layers at 44 cm and 31 cm above the bottom.

Table 5 The results of tracer tests for snowpacks on a slope and flat site. *HS* : snow depth. *L* : the distance of movement along slope. The values are average lengths from several test. The values in brackets indicate the maximum. *T* : the travel time of infiltration. The values are adjusted to correspond to the snow depth of 100 cm.

(1) slope

Date	*HS* cm	*L* cm	*T* min.
1992 4/26	91	95 (106)	140
1992 5/ 6	61	176 (230)	160

(2) Flat site

Date	*HS* cm	*T* min.
1992 5/ 7	97	140

Table 6 Comparison of the meltwater speeds along slope and vertical.

Date	Speed [cm/min.]	
	Vertical	Slope
1992 4/26	0.7	1.6
1992 5/ 6	0.6	1.7

This observation showed that the movement along slope affected the travel time little because the length of the movement along slope was small and the speed was much larger than vertical speed. Thus the travel time through the snowpack on a slope can be treated in the same manner as that on a flat site.

3. *Spatial distribution of snowmelt in the watershed*

The travel time through the snowpack varies depending on the snow depth in the watershed, as mentioned in the previous sections. However, this is true only when the snowmelt rate is the same everywhere. As shown in Figure 13 in chapter IV-1, the infiltration speed in a snowpack is highly dependent on the snowmelt rate. The snowmelt intensity distribution must be known in order to obtain the spatial distribution of the infiltration speed for the snowpack.

Figure 32 shows the lowering of snow surface at two sites (at the top and at the east ridge at an altitude of 375 m.a.s.l.) in the watershed compared with that at the base station. This comparison did not include days of snowfall. As shown in the figure, the values at each site were nearly equal to each other. The surface density of the snowpack was nearly constant in the entire watershed, and the snowmelt rates were also equal. The results at the other sites were similar to the result of Figure 32. Consequently the snowmelt occurs uniformly at any site in the watershed on fine days during the active snowmelt season. Motoyama(1986) obtained similar results using the heat balance method for the adjacent watershed.

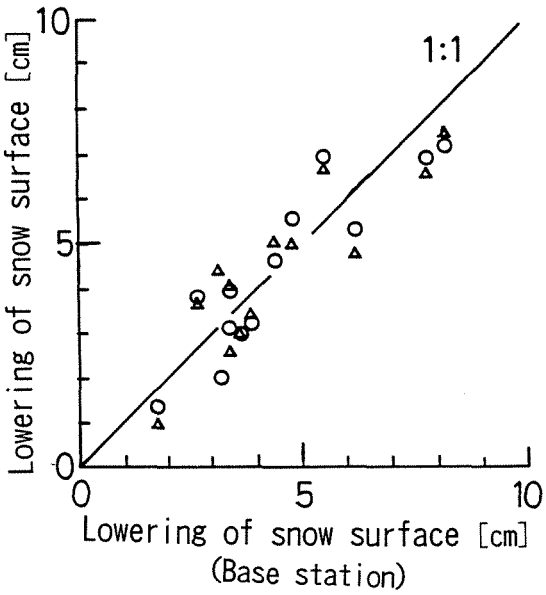

Figure 32 Comparison of the daily lowering of the snow surface at two sites in the watershed with that at the base station from April 11 to April 24, 1989, except for snowy days. Open circles : top station. Triangles : 375m a.s.l. on east ridge.

This chapter concludes that the travel time through the snowpack changes depending only on the snow depth in the watershed, because the infiltration speed in the snowpack is constant and the snowmelt is uniform. Therefore if we know the distribution of the snow depth in the watershed, the infiltration model (chapter IV-4) can be applied to the watershed.

VI. Application of the infiltration model to the watershed

The meltwater infiltration model developed for the snowpack at a flat site can be extended to the watershed if we know the distribution of snow depth, as described in the previous chapter. This chapter discusses the combined model of the infiltration model with a kinematic wave model, which calculates the processes in soil and river, in order to simulate the hydrograph in the river.

1. *Model of the watershed*

In order to simulate the discharge at the outlet of the watershed, a characteristic topography of the watershed has to be described. Figure 33 shows snow depth distribution with altitude. In this watershed, the snow depth was nearly constant under 400 m a.s.l., and it increases with altitude over this altitude. The character of the snow depth distribution was observed every year. The watershed was divided into two parts at the altitude of 400 m a.s.l. and simplified to two rectangular watersheds, as shown in Figure 34. The length of the river, and the steepness and size of the slope are determined by the topographical map. The snow depth in the upstream part is assumed to be the same as that at the top station. In the downstream part, it is assumed to be the same as that at the base station.

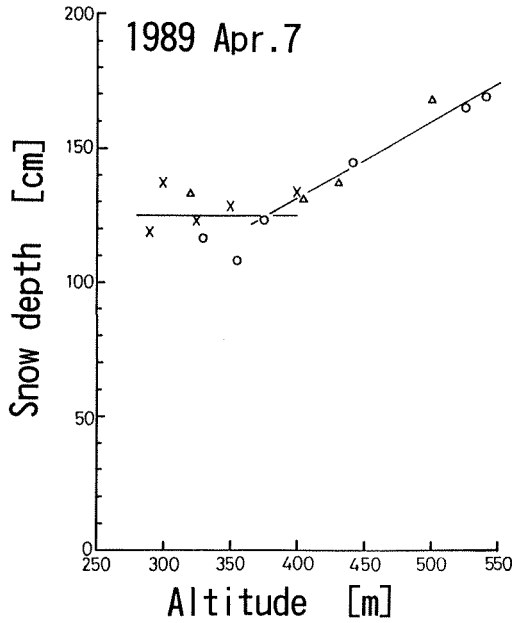

Figure 33 Altitudinal distribution of snow depth. Circles : east ridge. Triangles : west ridge. Crosses : valley.

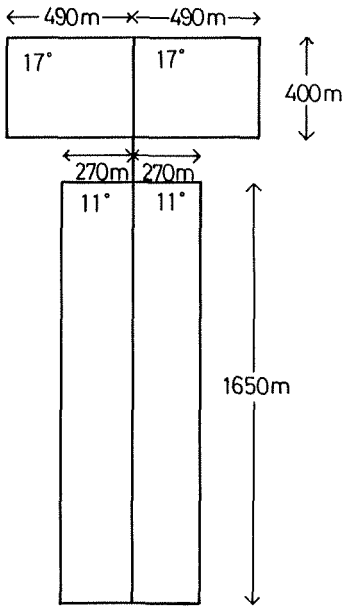

Figure 34 Watershed model. Upper and lower rectangls indicate upstream and downstream parts.

2. Simulation of hydrograph

1) *Slope flow and stream flow*

The present simulation consists of the processes in which water flows on the slope, collecting the water discharged from the bottom of the snowpack, and in which water flows in the river, collecting the water discharged from the end of slope. The infiltration model developed in chapter IV-4 calculates the discharge at the bottom of the snowpack. In the following, the slope flow and the stream flow for calculation will be described.

The equations of the motion and the continuity of the water on the slope are as follows.

$$h = kq^p, \tag{19}$$

$$\frac{\partial h}{\partial t} + \frac{\partial q}{\partial x} = q_*, \tag{20}$$

where h is the water depth, q the quantity of water in a unit width, and q_* the discharge at the bottom of the snowpack. t is the time and x is the distance from the top of the slope. k and p are constants which determine the characteristics of the slope flow. Equation (19) assumes a uniform sheet flow. If the flow is overland flow or groundwater flow, Manning's formula and Darcy's law determine the values of p and k. In this watershed, Kobayashi

(1985, 1986) reported that underground flow was dominant for snowmelt runoff, but the characteristic of this flow was not well understood. This study adopts 0.8 and 6.0 for p and k for both parts of the watershed according to a trial and error method. These values are not changed with year or period.

If the stream flow is regarded as a Manning's flow, the equations of the motion and the continuity are as follows.

$$A = KQ^P, \tag{21}$$

$$\frac{\partial A}{\partial t} + \frac{\partial Q}{\partial X} = Q_*, \tag{22}$$

where A is the cross sectional area of flow, Q the discharge in the stream, and Q_* the discharge at the end of the slope. t is the time and X is the distance from the top of stream. K and P are constants which determine the characteristics of stream flow, and these are written as,

$$K = \frac{n}{K_1^{\frac{2}{3}} I^{\frac{1}{2}}}, \tag{23}$$

$$P = \frac{3}{3 + 2z}, \tag{24}$$

where n is Manning's roughness in stream, I the gradient of the stream bed, and K_1 and z are led from the relationship between hydraulic depth R and the cross sectional area of stream A as written in the following.

$$R = K_1 A^z. \tag{25}$$

On the basis of the observation made by Ishii (1994), this calculation adopts 1.4 of P and 0.7 of K for the upstream, and 1.5 and 0.7 for the downstream.

The slope and stream flows can be calculated by the kinematic wave method using the equations and the values mentioned above. The simulation result is the direct runoff in the hydrograph. The total runoff consists of the direct runoff, which is characterized by a quick response, and the base flow, which had a slower response. The direct runoff in a hydrograph is the part above the line which connects the point of minimum runoff of one day with that of the next day. The part lower than this line is regarded as a base flow.

The input for the model calculation is the discharge at the bottom of the snowpack, which is calculated by the infiltration model described earlier. The daily discharge at the bottom of the snowpack is larger than the daily direct runoff. Therefore, the discharge for the input is adjusted so that its daily total becomes equal to the daily direct discharge by multiplying the coefficient by the hourly value of the discharge for the input.

2) *Results*

Figure 35 shows three results. The upper figure in each figure shows the snowmelt at the base station, since the snowmelt rate is uniform all over the watershed. The middle figure shows the calculated discharge at the bottom of the snowpack. The initiation of discharge in the region of the upstream is later than that in the downstream due to the thicker snowpack. The lower figure shows the hydrograph at the outlet of the watershed. The calculated discharges simulated the observations well for not only a single year but for all years.

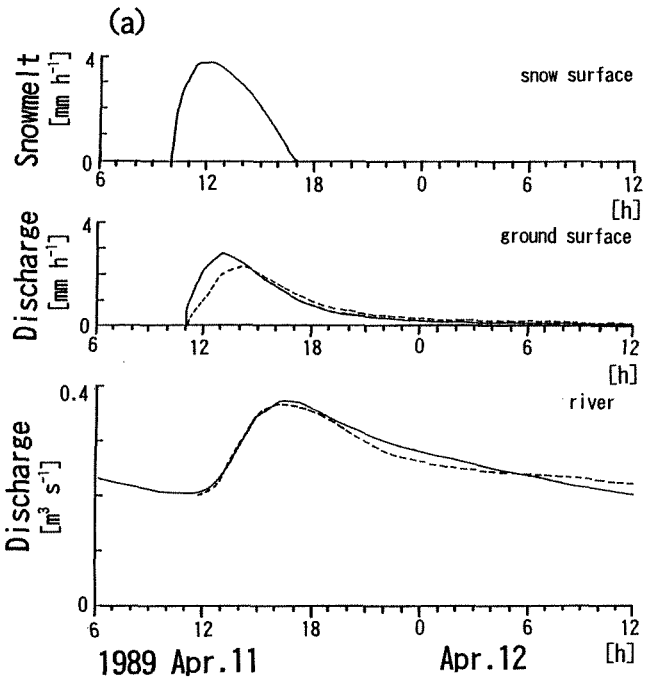

Figure 35 (a) Snowmelt, the discharge at the bottom of the snowpack, and runoff in the river. The upper figure shows the observed snowmelt at the base station. The middle figure shows the calculated discharges at the bottom of the snowpacks for the downstream area (solid line) and calculated discharge for the upstream area (broken line). The lower figure shows observed discharge (solid line) and calculated discharge (broken line) in the river. Snow depths were 88 cm in the downstream area and 143 cm in the upstream area.

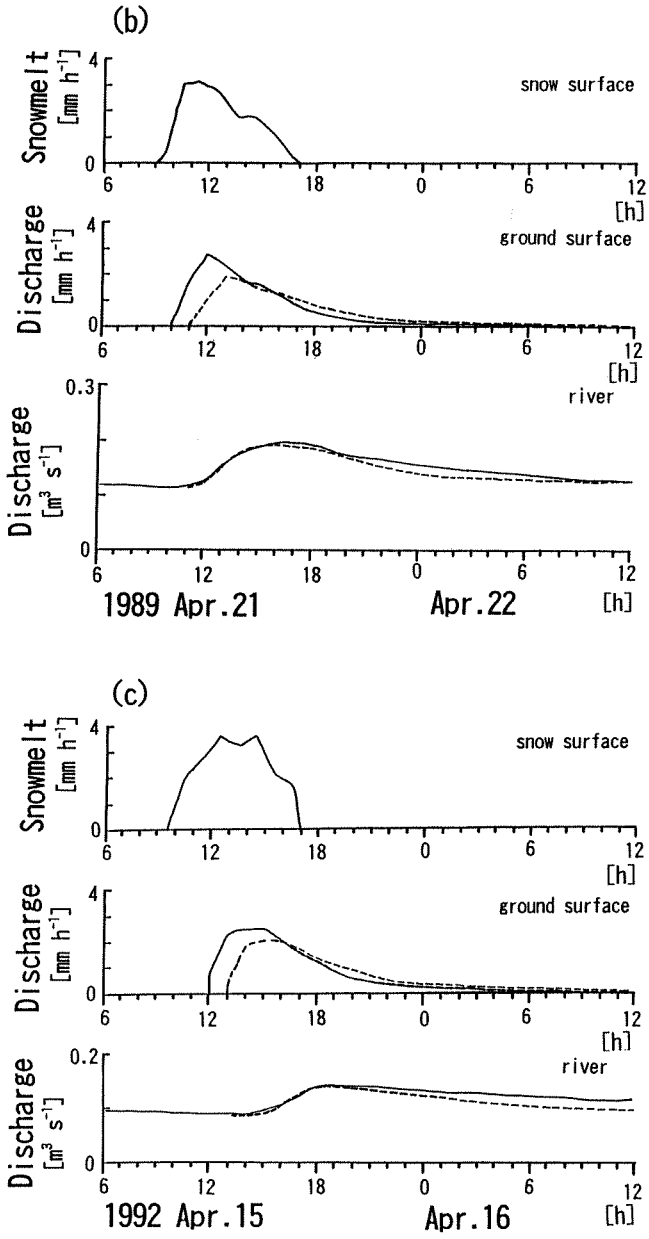

Figure 35 (b)-(c) The notations are the same as in Figure 35 (a). (b) Snow depths were 42 cm in the downstream area and 100 cm in the upstream area. (c) Snow depths were 88 cm in the downstream area and 127 cm in the upstream area.

Since the same value of p and k were used in the simulation, the characteristics of slope flow did not change with year or period. That means that the travel time is constant from the bottom of the snowpack to the river, which is shown in Figure 9 (chapter III-2).

In snowmelt runoff, the infiltration through the snowpack delayed notably the discharge to the river. The peak time in the calculated discharge is compared with the snow depth in the same manner in Figure 8 in chapter III-2 (Figure 36). Figure 36 shows that peak time becomes earlier with decreasing snow depth. The lines in Figure 36 are the same lines in Figure 8 (chapter III-2). This simulation described the yearly differences as well.

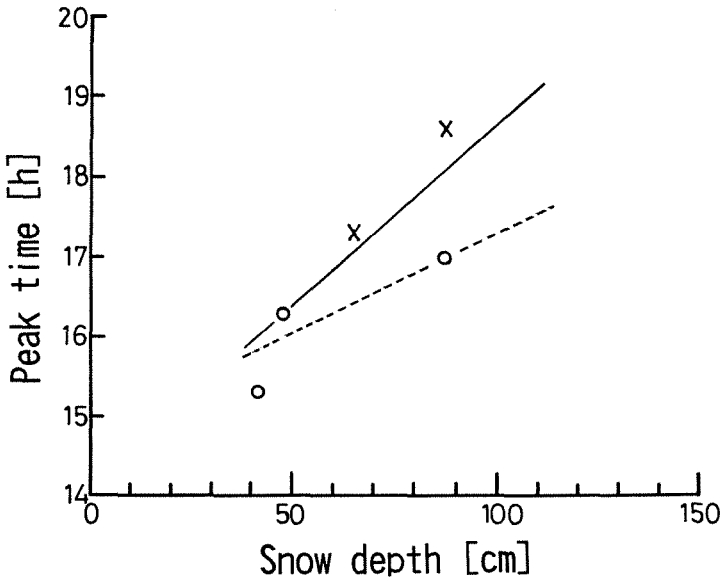

Figure 36 Relationship between the time of calculated peak runoff and the snow depth at the base station. Circles : 1989. Crosses : 1992. Solid and broken lines are the lines for 1992 and for 1989, which were drawn based on the observed results in Figure 8.

In this chapter, the runoff was simulated by the infiltration model and the runoff model of the kinematic wave method considering the distribution of snow depth in the watershed. The results simulated the hydrograph well and showed the observed yearly differences in the time of peak discharge.

VII. Summary

This paper discussed the snowmelt runoff process, particularly the meltwater infiltration through the snowpack, and presented the characteristics of the infiltration as the delayed mechanism of runoff response. The summary is as follows.

(1) Runoff coefficient for a few days did not change during the active snowmelt season and it was close to the runoff coefficient for the entire snowmelt season. It leads to the conclusion that meltwater was discharged into the river without storage in the snowpack.

(2) The time of the peak runoff became earlier with decreasing snow depth, and it is different from year to year.

(3) The yearly difference of the time of the peak runoff was caused by the difference in the travel time in the snowpack. The travel time in soil was nearly constant.

(4) The apparent speed of meltwater infiltration in the years with a large number of ice layers in the snowpack was larger than that in the years with a small number of ice layers.

(5) We hypothesized that the above phenomena was caused because the meltwater concentrated at the ice layers and the concentrated meltwater moved at a higher speed. The concentrated flows were observed with the multi-compartment lysimeter. On the basis of these observations, the infiltration model of the concentrated flow was developed. This model could simulate the observed hydrographs very well and could show the yearly difference in the speed.

(6) The comparison of the infiltration between the sites with different altitudes and different topography shows that the travel time in the snowpack alters depending only on the snow depth in the watershed.

(7) The infiltration model was applied to the watershed considering the distribution of snow depth, and the simulation of runoff was made with the kinematic wave method. The results simulated the hydrograph well and presented the observed yearly difference in runoff response.

Acknowledgments

The author is grateful to the staff members of the Uryu Experimental Forest of Hokkaido University for their help in this study, Mr. S. Matsumoto of the Institute of Low Temperature Science (I.L.T.S.) for enthusiasm in making the lysimeters, and Miss Y. Takeuchi and Mr. H. Nakabayashi, the graduate students of I.L.T.S., for their assistance of the observations. The author also wishes to thank Profs. K. Fujino, E. Akitaya of I.L.T.S. ; and Prof. K. Nakao of Faculty of Science, Hokkaido University for helpful advice and useful suggestions, and Drs. Y. Ishii, Y. Kodama, N. Ishikawa and Prof. D. Kobayashi of I.L.T.S. for

continuous discussions and encouragement.

References

Colbeck S.C. 1972 A theory of meltwater percolation in snow. *J. Glaciol.*, **11**, 369–385.

Colbeck S.C. 1978 The physical aspects of water flow through snow. *Advances in Hydroscience*, **11**, 37–45.

Colbeck S.C. 1979 Water flow through heterogeneous snow. *Cold Reg. Sci. and Technol.*, **1**, 37–45.

Dunne T., Price A.G. and Colbeck S.C. 1976 The generation of runoff from subarctic snowpack. *Water Resour. Res.*, **12**, 677–685.

Fujino K. 1968 Measurement of flow down speed of melt water in snow cover. *Low Temp. Sci., Ser.* **A, 26**, 87–100 (in Japanese with English summary).

Fujino K. 1971 Measurement of flow down speed of melt water in snow cover. II.—Flow of melt water in snow cover on a slope—. *Low Temp. Sci., Ser.* **A, 26**, 151–158 (in Japanese with English summary).

Furbish D. J. 1988 The influence of ice layers on the travel time of meltwater flow through a snowpack. *Arctic and Alpine Res.*, **20**, 265–272.

Hamada K., Kodama Y. and Kobayashi D. 1988 Meltwater percolation through snow cover I. *Low Temp. Sci., Ser.* **A, 47**, 89–101 (in Japanese with English summary).

Ishii Y. 1994 Personal communication.

Ishikawa N., Kobayashi S. and Kojima K. 1982 Measurement of sensible heat flux in the snowmelting season I. *Low Temp. Sci., Ser.* **A, 41**, 109–116 (in Japanese with English summary).

Jordan P. 1983a Meltwater movement in a deep snowpack. 1. Field observations. *Water Resour. Res.*, **19**, 971–978.

Jordan P. 1983b Meltwater movement in a deep snowpack. 2. Simulation model. *Water Resour. Res.*, **19**, 979–985.

Kobayashi D. 1973 Flow down speed of melt water in snow cover I. *Low Temp. Sci., Ser.* **A, 31**, 135–142 (in Japanese with English summary).

Kobayashi D. and Motoyama H. 1985 Effect of snow cover on time lag of runoff from a watershed. *Annals of Glaciol.*, **6**, 123–125.

Kobayashi D. 1985 Separation of the snowmelt hydrograph by stream temperature. *J. Hydrol.*, **76**, 155–162.

Kobayashi D. 1986 Separation of the snowmelt hydrograph by stream conductance. *J. Hydrol.*, **84**, 157–165.

Maeno N. and Fukuda M. 1986 Seppyô no kôzô to bussei. Kokinsyoin, 209pp (in Japanese).

Marsh P. and Woo M.K. 1984a Wetting front advance and freezing in meltwater within a snow cover. 1. Observations in the Canadian Arctic. *Water Resour. Res.*, **20**, 1853–1864.

Marsh P. and Woo M.K. 1984b Wetting front advance and freezing in meltwater within a snow cover. 2. A simulation model. *Water Resour. Res.*, **20**, 1865–1874.

Marsh P. and Woo M.K. 1985 Meltwater movement in natural heterogeneous snow covers. *Water Resour. Res.*, **21**, 1710–1716.

Motoyama H., Kobayashi D. and Kojima K. 1983 Water balance at a small watershed during the snowmelt season I. *Low Temp. Sci., Ser.* **A, 42**, 123–133 (in Japanese with English summary).

Motoyama H. 1983 Studies of basin heat balance and snowmelt runoff models. *Contri. from the Inst. of Low Temp. Sci., Ser* **A., 35**, 1–53.

Shimizu H. 1970 Air permeability of deposited snow. *Contri. from the Inst. of Low Temp. Sci,,*

Ser **A.**, **22**, 1−32.
Wakahama G. 1963 The infiltration of melt water into snow cover I. *Low Temp. Sci., Ser.* **A**, **21**, 45−73 (in Japanese with English summary).
Wakahama G., Nakamura T. and Endo Y. 1968 Infiltration of melt water into snow cover II. *Low Temp. Sci., Ser.* **A**, **26**, 53−76 (in Japanese with English summary).
Wakahama G. 1968 Infiltration of melt water into snow cover III. Flowing down speed of melt water in a snow cover. *Low Temp. Sci., Ser.* **A**, **26**, 77−86 (in Japanese with English summary).
Wankiewicz A. 1978 Water pressure in ripe snowpacks. *Water Resour. Res.*, **14**, 593−600.
Yosida Z. 1965 Infiltration of melt water in snow cover. *Low Temp. Sci., Ser.* **A**, **23**, 1−16 (in Japanese with English summary).